Engineering and Technology Journal e-ISSN: 2456-3358
Volume 11 Issue 08 August-2026, Page No.-11072-11105
DOI: 10.47191/etj/v11i08.04, I.F. – 8.595


# Imaging and Convolution Neural Network for Surface Finish Quality Assurance on Assembly Line

**Ndifreke Ikemesit Effeng[1], Chikodili Martha Orazulume[2], Whyte Asukwo Akpan[3], Awaka-Ama Emediong Johnson[4], Victor Anso Amba[5], Iniobong Okon Nyah[6]**

[1]Department of Mechanical Engineering of Mechanical Engineering, Faculty of Engineering, University of Uyo, Akwa Ibom State, Nigeria

[2]Department of Electrical and Electronics Engineering, Faculty of Engineering, TopFaith, University Mkpatak, Akwa Ibom State, Nigeria

[3]Department of Mechanical Engineering, School of Engineering and Engineering Technology, Federal University of Technology, Ikot Abasi, Nigeria.

[4]Department of Mechanical Engineering of Mechanical Engineering, Faculty of Engineering, University of Uyo, Akwa Ibom State, Nigeria

[5]Department of Mechanical Engineering of Mechanical Engineering, Faculty of Engineering, University of Uyo, Akwa Ibom State, Nigeria

[6]Department of Mechanical Engineering of Mechanical Engineering, Faculty of Engineering, University of Uyo, Akwa Ibom State, Nigeria

**ABSTRACT:** Surface finish of a product is among one of the important parameters of manufacturing process consideration. A product no matter the configuration without a good surface finish will not wholly be acceptable by the customers unless the roughness is part of engineering consideration. On the assemble line, inspection is usually carried out to check if the product has met its surface finish requirements. Such inspection includes sampling techniques such as single and double sampling etc. These techniques are cumbersome, costly, and sometimes unable to completely uncover all the defects in a batch. For a continuous production line, therefore, it is desirable to deploy an alternative and superior method that can reduce the number of defects, easy to apply, less expensive and allow flow with manufacturing process. This was accomplished by classifying flaws on metal surfaces and detecting roughness on them using Convolution Neural Networks (CNN). 1800 images of metal surface flaws were gathered to create this dataset. With three hundred images of metal surfaces for each of the six defects: pitted surfaces, patches, inclusions, crazing, rolled in scales, and scratches-the flaws were categorized. There were roughly 1620 photos which was trained (90%) and about 180 pictures that was used in model testing (10%). With the model developed images of any other metal surface can be taken on the production line and compare with the established model.

**KEYWORDS:** Assembly line, classification, CNN, Imaging, roughness, surface finish, testing.

## INTRODUCTION

Surface finish involves the process of altering a material's surface by adding, removing, or reshaping [1]. These measures are used to ensure a smooth surface, great accuracy, aesthetic appearance, or protective coating. Surface roughness is typically measured perpendicular to the lay direction by an instrument known as profilometer [2]. The relationship between roughness and smoothness of a component's surface is called surface finish [3]. Since surface finishing is a product of machining operation, it follows that surface finishing has a direct correlation with the type of machining operation used, tool and other machining parameters. Surface roughness occurs because of poor choice of cutting speed, feed rate and depth of cut - with the result being localized irregularities of the surfaces of the material. It is worth noting that some applications need close tolerance which demands that parts be produced as close to the design specification as possible. Hence, in such cases, it becomes necessary that checks be put in place to ensure that the surfaces are smooth and close to the laid-down dimensions as possible.

Also, a good finish ensures a minimal resistance between the two moving parts and wear between such moving parts is also minimized, hence such parts have longer life and less unexpected failure rate during continuous operation [3]. Other properties such as heat transmission, light reflection, ability to hold lubricants are also affected due to quality of machined surface of a part [3]. Figure 1 (a) shows the surface finish profile.

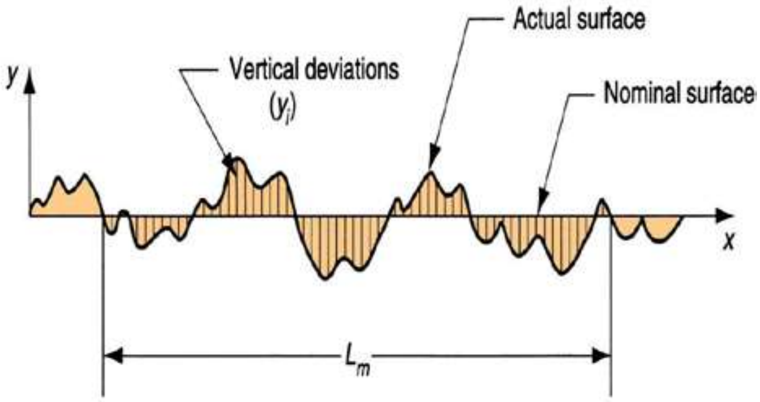


**Figure 1 (a): Surface finish profile [4]**

Roughness, waviness, and form are the different categories of surface finish criteria. According to [5] irregularity in part’s outward finishing, or just irregularity, is a measurement of all the dispersed part’s outward abnormalities. Either a non-contact method or a contact type meter is used to detect surface roughness. Tracing the contact probe of roughness meter, across the surface of the object to be evaluated is an operation that involves touch. In non-contact method, illumination is used instead of the probe.

A standard Surface of a material is described as overall contour of outer layers omitting or completely disregarding waviness and roughness.

Nonetheless, a material's outer finishing can be determined by its form, waviness, roughness, or a mix of two or three of these characteristics. The surface roughness parameters are shown in Figure 1(b).

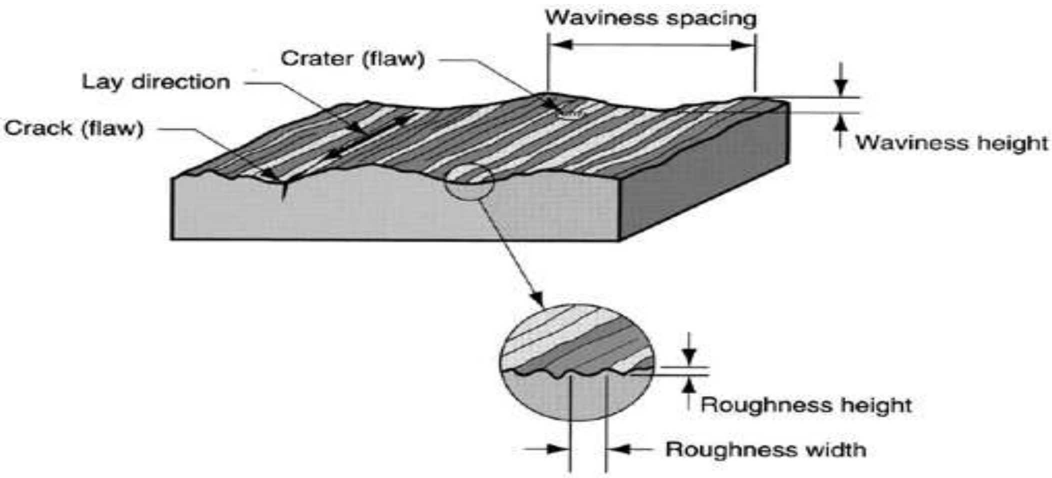


**Figure 1(b): Surface finish profile showing roughness parameters** [4]

Ra has been in frequent use as irregularity parameter, albeit this is usually due to historical reasons rather than any specific worth as roughness meters that were used in the early days was able to measure only Ra [6].

A parts outer finish definitions are divided into three categories: hybrid, spacing, and amplitude variables.

Most of the time, amplitude parameters quantify surface variations in terms of vertical properties. A few of these metrics are:

(i) Roughness Mean Arithmetic value (Ra)**:**

Gauges how far the irregularity deviates from average.

$$Ra = \frac{1}{l}\int_0^l |z(x)|\,dx$$

Equation 1

where; z(x) is a roughness profile of length L.

(ii) Roughness Root Mean Value (Rq):

$$Rq = \sqrt{\frac{1}{l}\int_0^l z^2(x)\,dx}$$

Equation 2

**Value**

(iii) Maximum profile valley depth (Rv) is the greatest depth of the outline within the total length under consideration that is below the average line.

$$Rvi = |\min z(x)| \qquad \text{Equation 3}$$

$$Rv = \frac{\sum_{i=1}^{n} Rvi}{n} \qquad \text{Equation 4}$$

where: Rvi is the maximum debts of profile below the mean line.

Spacing Parameters: These parameters define surface in terms of the distance. These parameters are:

(i) Mean Spacing (Rsm): This is the average spacing between profile elements at the mean line within the chosen length.

(ii) Peak Count (Rpc): These measures how many irregularity profile peaks extend above the mean line per unit of distance.

(iii) The Highest Spot Count (HSC): According to [7] this index is the numeral figure of greatest patches in the outline per section within the length under consideration that exceeds the average line - that exceeds the line which is parallel to the average line.

(iv) Mean spacing of Adjacent local Peaks (S): [7] it represents profile's average separation of nearby regional high spot as determined within the line under consideration.

(v) Hybrid-Parameters: These variables incorporate amplitude and spacing information

Classification of surface techniques used are:

(i) Centre line Average (CLA): This requires drawing a average line in the surface outline's direction. It is the average, as the name suggests, indicating that the areas uppermost and lowermost regions are roughly even-handed. Thus, the mean of the vertical points is computed by dividing sampling length by the total of the areas above and below the line. Equations 5, 6, and 7 show them, in that order [8].

$$Ha = A/L = ((A+A+A) + (B+B))/L \qquad \text{Equation 5}$$

$$CLA = HA\,(VXH)X1000\pi m \qquad \text{Equation 6}$$

$$Ra = \{ (A+A+A)+(B+B)L \} x1000\pi m \qquad \text{Equation 7}$$

where: A and B are portions above and below the mean line respectively.

(ii) Root Mean Square Method: this involves taking geometric mean using profile's y-axis around mean line [8] states that if measurements are taken from the surface profile's points to the mean line above and below.

(iii) Ten Points Heights Method: This is a border drawn side by side to the average horizontal border without exceeding the outline is employed in estimating the mean difference in the finest high and low point troughs of textural features within the length under consideration.

Table 1 shows the interpretation of surface roughness symbols.

**Table 1: Interpretation of Roughness Symbols**

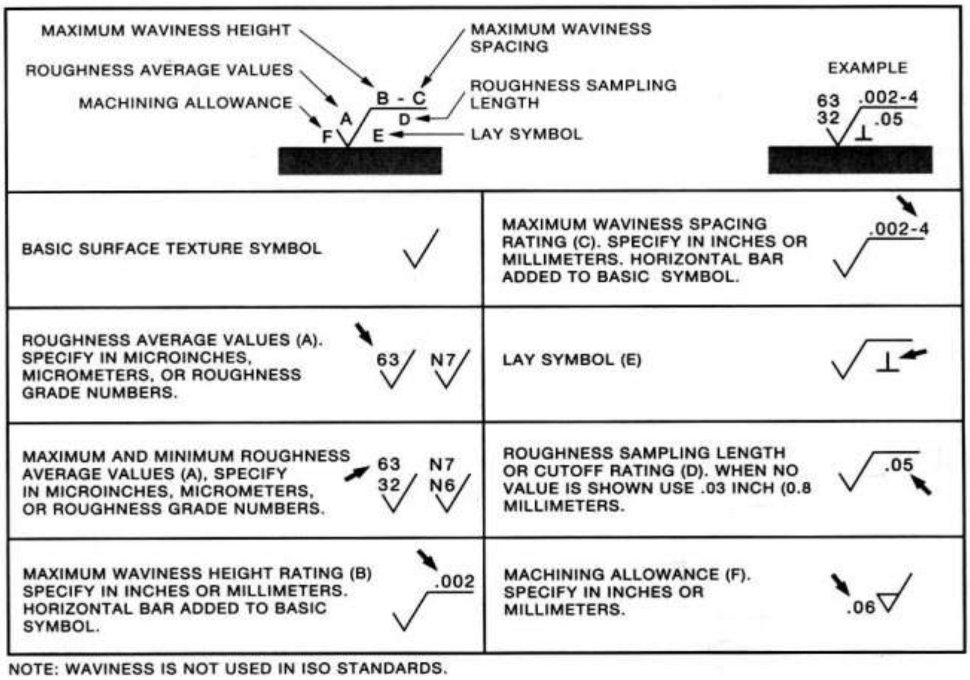


**Source**: [9]

Table 2 shows roughness parameters and the grading system.

**Table 2: Roughness Parameters and Grading**

| Ra micrometer μ m | Ra micro-inch μ in | Roughness Grade Numbers (New)** | Roughness Grade Numbers (Old)*** | $R_t$ | √(Ra) | Old Style | American standard |
|---|---|---|---|---|---|---|---|
| 50 | 2000 | N12 | | | | | |
| 25 | 1000 | N11 | ▽ | | | | |
| 12.5 | 500 | N10 | | | | | |
| 6.3 | 250 | N9 | | 32 | 6.3 ▽√ | 32 ▽ | 250√ |
| 3.2 | 125 | N8 | ▽▽ | 16 | 3.2 ▽√ | ▽▽ | 125√ |
| 1.6 | 63 | N7 | | 8 | 1.6 ▽√ | 8 ▽▽ | 63√ |
| 0.8 | 32 | N6 | | 4 | 0.8 ▽√ | ▽▽▽ | 32√ |
| 0.4 | 16 | N5 | ▽▽▽ | 2 | 0.4 ▽√ | 2 ▽▽▽ | 16√ |
| 0.2 | 8 | N4 | | 1 | 0.2 ▽√ | ▽▽▽▽ | 8√ |
| 0.1 | 4 | N3 | | 0.5 | 0.1 ▽√ | 0.5 ▽▽▽▽ | 4√ |
| 0.05 | 2 | N2 | ▽▽▽▽ | 0.25 | 0.05 ▽√ | 0.25 ▽▽▽▽ | 2√ |
| 0.025 | 1 | N1 | | | | | |

[9]

Surface parameters can be evaluated by comparing the values obtained with the standard values. Table 3 shows the international standard organization conversion chat for surface finish.

**Table 3: Surface Finish Conversion Chart**

Surface Finish Conversion Chart

| N | Rt | Ra | CLA | RMS | Cut-off length Inches | mm |
|---|---|---|---|---|---|---|
| 1. | 0.3 | 0.025 | 1 | 1.1 | 0.003 | 0.08 |
| 2. | 0.5 | 0.05 | 2 | 2.2 | 0.01 | 0.25 |
| 3. | 0.8 | 0.1 | 4 | 4.4 | 0.01 | 0.25 |
| 4. | 1.2 | 0.2 | 8 | 8.8 | 0.01 | 0.25 |
| 5. | 2.0 | 0.4 | 16 | 17.6 | 0.01 | 0.25 |
| 6. | 4.0 | 0.8 | 32 | 35.2 | 0.03 | 0.8 |
| 7. | 8.0 | 1.6 | 63 | 64.3 | 0.03 | 0.8 |
| 8. | 13 | 3.2 | 125 | 137.5 | 0.1 | 2.5 |
| 9. | 25 | 6.3 | 250 | 275 | 0.1 | 2.5 |
| 10. | 50 | 12.5 | 500 | 550 | 0.1 | 2.5 |
| 11. | 100 | 25.0 | 1,000 | 1,100 | 0.3 | 8.0 |
| 12. | 200 | 50.0 | 2,000 | 2,200 | 0.3 | 8.0 |

*N = New ISO scale numbers*
*Rt = Roughness, total in microns*
*CLA = Center line average in microinches*
*RMS = Root mean square in microinches*
*Ra = Roughness, average in microns*

**[9]**

The reproduction of man’s intellectual processes using devices, especially PC, is called artificial intelligence. This includes the ability to recognize spoken words, machine-vision, ability to process dialects, to mention but a few.

Artificial intelligence, overall, involve developing a PCs using propositional computing which enables the system to make decisive steps, translate articulations, recognize voices and analyse visuals. Logical thinking, cognitive applications, organizing, tuition abilities, ability in processing articulations, vision, and device movement and manipulation are among the objectives of artificial intelligence research.

But the true test of artificial intelligence is how well computer-aided programming codes and instructions imitate the workings of the human brain, guaranteeing that decisions are made and carried out in a way that makes sense. Overall, AI-system functions through the learning process where named-information are properly analysed to learn and extract the features in the information, to make projections into the future [10],[11]. The objective of this research is to apply imaging with AI to obtain surface finish of part or component for quality assurance on an assembly line.

## 2.0 METHODOLOGY

Datasets of images was captured, and an algorithm was trained as part of the Convolution Neural Network process, which enables the model in using the data that has been subjected to training to identify instances in which the standard deviated from the intended standard.

The level of precision, which is a measure of the efficiency of the model, and mean error were assessed after the model underwent testing. By establishing a correlation between the trained dataset and any given image, the system was able to determine if an image was precise or false.

This was accomplished by classifying flaws on metal surfaces and detecting roughness on them using Convolution Neural Networks (CNN). 1800 images of metal surface flaws were gathered to create this dataset. With three hundred images of metal surfaces for each of the six defects—pitted surfaces, patches, inclusions, crazing, rolled in scales, and scratches—the flaws were categorized.

There were roughly 1620 photos which was trained (90%) and about 180 pictures that was used in model testing (10%). Figure shows the flowchart of the algorithm.

The computations are performed based on the layers displayed thus:

(i) Data- Input: This represents information entry into the model. It is the image's matrix-operation of the pixels.

The entry dimensions of the images are (200, 200, 3), with the first, second and third values representing the image's height, breadth, and the number of RGB colour channels respectively. The sum of the input learnable components in the input phase is therefore obtained from the following: input neurons = H * W * channels. This is correspondingly evaluated using the dimensions given above to obtain #n a value of 120,000.

ii) Convolution-phase: Here, outputs connected to the input dataset were computed. Input volume is calculated by taking the scalar products of the resultant input phase operation and the field which receives it and connecting layers.

Filters make up the convolution phase. It is important to note that every convolution filter is a representation of the features, or dataset pixel information, that the algorithm learns, in carrying out calculations. 32 filters make up the first convolutional layer. (5, 5) is the kernel size. With the padding placed at "same," the geometrical orientation of the output will match that of the input. The kernel increases by a pixel with respect to time when the stride value is 1. Each filter's parameter count is determined thus:

((5 * 5 * 3)+ 1). The result is multiplied by 32. This gives a total param of 2432. This represents the number of params in each filter.

Consequently, 32 * 2432 = 77,824. This represent the params in the first phase of this layer.

iii) Pooling Layer: This layer sits between the fully connected layer and the convolution layer. One subsampling method which enables data generalization to be achieved is max pooling. Maximum pooling helps in obtaining input with fewer dimensions, hence in ensuring reduction of overfitting. Where a relation or model fits in and is nearly like a small collection of processed information, a model error known as overfitting occurs, making it difficult for the system to make deductions on a larger set. When a model performs well during training but poorly during testing, it is considered overfitted because it lacks the ability to learn and remember.

The largest values of the input information are represented by the maximum pixel dimensions chosen in this case of maximum pooling. The computation of the values results in a downsampled result, which lowers the dimensions of the input data. Reducing the parameters required is aided by maximum pooling. The maximum pooling phase helps in reducing the geometrical parameters by a factor of two. Given that the dimension is (2, 2), the largest param inside a 2x2 axis is chosen. The number of neurons remained the same because the pooling layer does not contribute any new parameters.

(iv) Pooling and Convolutional Layer:

The pattern of the second set of convolutional layers is comparable to that of the first. Each of the 64 filters in the second set has a kernel size of (3, 3). The padding is "same," and the stride is 1. Consequently, each filter has the following amount of params: Params of each filter = (3 * 3 * 32). The result is added to 1 and multiplied by 64. This gives a total params of 18,496.

The next phase of convolution has 1,181,184 parameters in total, which is obtained by multiplying 64 by 18,496.

The spatial dimensions are further reduced by a factor of two by the second max pooling layer.

(v) Dense Layer: A dense layer comprising 256 neurons is inserted after the convolutional and pooling layers. The output of the preceding layer, a tensor of shape (25, 25, 128), serves as the input for these dense layers. This dense layer's parameter count is determined as follows:

(Input shape * 256) + 256 = (25 * 25 * 128 * 256) + 256 = 20,480,256. This is the number of parameters.

(vi) Flattening Layer: This layer creates a 1D vector from the dimensional arrays of the preceding phase, with the size 25 by 25 and 128. The product of the dimensions determines the sum of learning activators in the flattening stage:

In the flattening layer, there are 80,000 neurons (25 x 25 * 128).

The information of the phase sizes and params in the specified system structure are provided by these computations.

The term "epoch" describes the iterative learning process that the system underwent when the algorithm was applied to the learning set. Since iteration (Epoch) is a single full dataset training cycle, the total epoch count indicates how many times the dataset was trained using the codes (algorithm).

Therefore, the learning period was repeated 150 times to ensure accuracy. The main goal of the iteration was to enable the achievement of a lower mean error value. This gives the machine the chance to learn the information given to the system and run the appropriate computations with it.

Furthermore, as was already discussed, the work was divided into batches, which were referred to as iterations—the number of batches required in finishing each epoch. The number of learning sets used in an Epoch is indicated by the batches here.

TensorFlow is a machine learning platform which has special features to give good user experience. This multidimensional array is employed for data storage. Features are the dimensions that are shown in the three-dimensional arrays; arrays are dataset for deep learning in AI. Based on Adam's Optimizer-Keras API standard, TensorFlow high level API are used. This makes quick prototyping and data training possible. Nonetheless, deep learning models may be created using the Keras high-level neural network framework, which is how the various layers were produced.

Additionally, the study developed models using Keras and the TensorFlow platform. Installing the Python application on the PC was one of the processes undertaken to configure the system. After that, the model was launched by installing TensorFlow, while also going through each of the following steps:

(i) Importing TensorFlow.
(ii) Downloading and preparing the training set.
(iii) Data Authentication
(iv) Convolutional Base Formation
(v) Insertion of a dense layer
(vi) Model development and the learning process
(vii) Analysis of the system efficiency.

Figure 1(c) shows a flow chart of the CNN algorithm for the model.

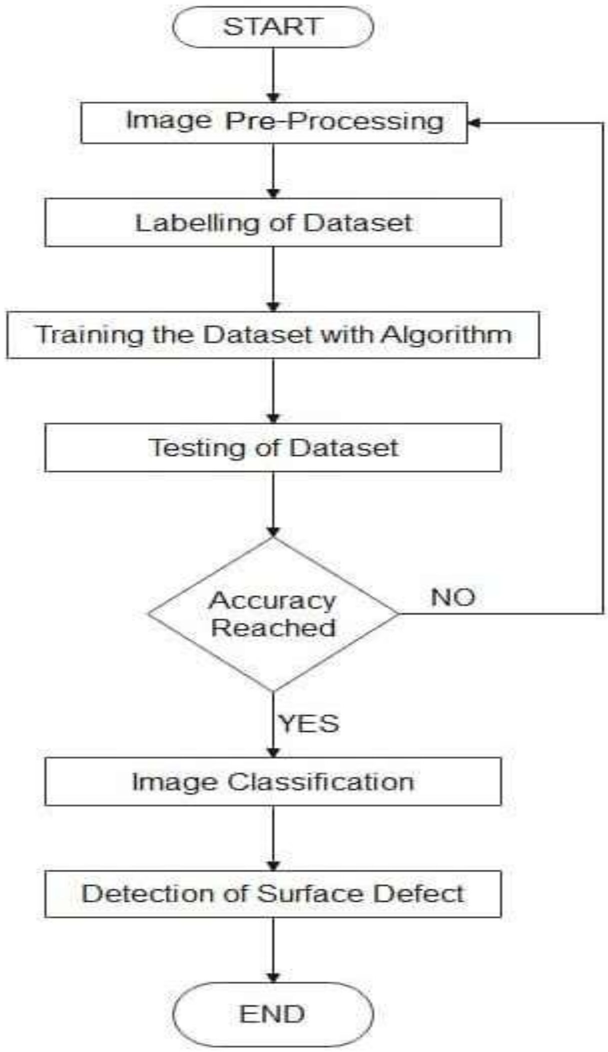


**Figure 1(c): Flowchart of CNN algorithm**

Figure 2 shows the Architecture of the CNN used.

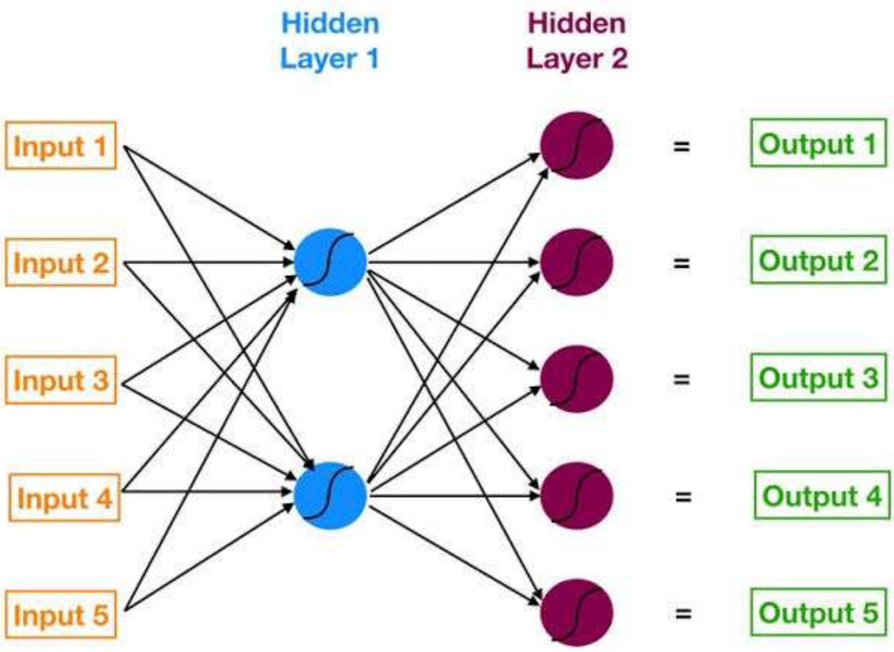


**Figure 2: Convolution Neural Network Structure**

**3.0 RESULTS AND DISCUSSION**

**3.1 Results**

The system was trained on six datasets, each comprising 300 photos, which represented six major defects on metal surfaces: patches, inclusions, crazing, pitted, scratches, and rolled-in-scales. As a result, neurons learnt and became more compliant with the algorithm, enabling the system to make predictions about the test samples' surface finish textures.

Nonetheless, the work had 150 epochs with a batch size of 24, a total of 70 batches were created. To assess the model's performance in each epoch, the model additionally evaluated the accuracy and error rates during dataset training and testing.

A call-back system was one of the mechanisms implemented to address any non-conforming behaviour during training. This also made sure that the training ended when the desired level of accuracy was reached.

Table 4 presents system accuracy losses and training validation for 150 epochs.

**Table 4: Data showing system Accuracy and Losses during training and validation of 150 Epochs.**

| Model Epoch(Iteration) | Model Accuracy | Model Losses | Accuracy during Validation | Losses during Validation | Implication |
|---|---|---|---|---|---|
| 1/150 | 0.1603 | 1.7797 | 0.1667 | 1.7713 | Increased |
| 2/150 | 0.2119 | 1.7457 | 0.3056 | 1.6982 | Increased |
| 3/150 | 0.3139 | 1.5992 | 0.3889 | 1.3885 | Increased |
| 4/150 | 0.3824 | 1.3815 | 0.6111 | 1.1440 | Increased |
| 5/150 | 0.4568 | 1.2480 | 0.6528 | 1.0781 | Increased |
| 6/150 | 0.5420 | 1.1024 | 0.6667 | 0.9732 | Increased |
| 7/150 | 0.5714 | 1.0227 | 0.7500 | 0.7730 | Increased |
| 8/150 | 0.6327 | 0.9455 | 0.8056 | 0.6975 | Increased |
| 9/150 | 0.6627 | 0.8606 | 0.8333 | 0.5891 | Increased |
| 10/150 | 0.6807 | 0.8279 | 0.8194 | 0.5571 | No increase from 0.8333 |
| 11/150 | 0.7197 | 0.7537 | 0.83333 | 0.5422 | No increase from 0.8333 |
| 12/150 | 0.7407 | 0.7111 | 0.8611 | 0.5101 | Increased |
| 13/150 | 0.7491 | 0.6814 | 0.7639 | 0.5678 | No increase from 0.8611 |
| 14/150 | 0.7695 | 0.6344 | 0.8889 | 0.3593 | Increased |
| 15/150 | 0.7785 | 0.5976 | 0.8750 | 0.4560 | No increase from 0.8889 |
| 16/150 | 0.8049 | 0.5711 | 0.7778 | 0.5837 | No increase from 0.8889 |

| | | | | | |
|---|---|---|---|---|---|
| 17/150 | 0.8109 | 0.5418 | 0.9028 | 0.3360 | Increased |
| 18/150 | 0.8115 | 0.5427 | 0.9306 | 0.2724 | Increased |
| 19/150 | 0.8427 | 0.4764 | 0.9306 | 0.2691 | No increase from 0.93056 |
| 20/150 | 0.8403 | 0.4612 | 0.9306 | 0.2738 | No increase from 0.93056 |
| 21/150 | 0.8427 | 0.4478 | 0.9028 | 0.3022 | No increase from 0.93056 |
| 22/150 | 0.8325 | 0.4715 | 0.9444 | 0.2247 | Increased |
| 23/150 | 0.8505 | 0.4203 | 0.9583 | 0.1903 | Increased |
| 24/150 | 0.8391 | 0.4673 | 0.8750 | 0.3550 | No increase from 0.9583 |
| 25/150 | 0.8691 | 0.3997 | 0.9167 | 0.2524 | No increase from 0.9583 |
| 26/150 | 0.8697 | 0.3840 | 0.9028 | 0.3192 | No increase from 0.9583 |
| 27/150 | 0.8764 | 0.3781 | 0.9444 | 0.1779 | No increase from 0.9583 |
| 28/150 | 0.8902 | 0.3372 | 0.9167 | 0.1944 | No increase from 0.9583 |
| 29/150 | 0.8836 | 0.3382 | 0.9306 | 0.1613 | No increase from 0.9583 |
| 30/150 | 0.8673 | 0.3686 | 0.9167 | 0.2057 | No increase from 0.9583 |
| 31/150 | 0.8547 | 0.4029 | 0.9444 | 0.1619 | No increase from 0.9583 |
| 32/150 | | 0.3425 | 0.9444 | 0.1428 | No improvement from 0.9583 |
| 33/150 | 0.8908 | 0.3410 | 0.9306 | 0.2084 | No increase from 0.9583 |
| 34/150 | 0.8884 | 0.3323 | 0.9306 | 0.1607 | No increase from 0.9583 |
| 35/150 | 0.9028 | 0.2854 | 0.9306 | 0.1737 | No increase from 0.9583 |
| 36/150 | 0.8992 | 0.2958 | 0.9028 | 0.2488 | No increase from 0.9583 |
| 37/150 | 0.8998 | 0.3020 | 0.9306 | 0.1696 | No increase from 0.9583 |
| 38/150 | 0.9064 | 0.2789 | 0.9583 | 0.1535 | No increase from 0.9583 |
| 39/150 | 0.9034 | 0.2840 | 0.9583 | 0.1278 | No increase from 0.9583 |
| 40/150 | 0.9076 | 0.2825 | 0.9444 | 0.1141 | No increase from 0.9583 |
| 41/150 | 0.8980 | 0.2959 | 0.9306 | 0.1510 | No increase from 0.9583 |
| 42/150 | 0.9118 | 0.2582 | 0.9583 | 0.0974 | No increase from 0.9583 |
| 43/150 | 0.9004 | 0.2784 | 0.9306 | 0.1259 | No increase from 0.9583 |
| 44/150 | 0.9154 | 0.2461 | 0.9444 | 0.1954 | No increase from 0.9583 |
| 45/150 | 0.9112 | 0.2545 | 0.9444 | 0.1336 | No increase from 0.9583 |
| 46/150 | 0.9202 | 0.2594 | 0.9583 | 0.1410 | No increase from 0.9583 |
| 47/150 | 0.9112 | 0.2466 | 0.9583 | 0.0961 | No increase from 0.9583 |
| 48/150 | 0.9160 | 0.2341 | 0.9444 | 0.1977 | No increase from 0.9583 |
| 49/150 | 0.9250 | 0.2422 | 0.9306 | 0.2139 | No increase from 0.9583 |
| 50/150 | 0.9214 | 0.2248 | 0.9722 | 0.0894 | Increased |
| 140/150 | 0.9712 | 0.0873 | 1.0000 | 0.0085 | Increased |
| 141/150 | 0.9730 | 0.0844 | 1.0000 | 0.0152 | Increased |
| 142/150 | 0.9784 | 0.0729 | 0.9306 | 0.3097 | No increase from 1.000 |
| 143/150 | 0.9790 | 0.0725 | 1.0000 | 0.0080 | Increased |
| 144/150 | 0.9706 | 0.0853 | 0.9722 | 0.1111 | No increase from 1.000 |
| 145/150 | 0.9694 | 0.0958 | 1.0000 | 0.0071 | Increased |
| 146/150 | 0.9610 | 0.1065 | 0.9722 | 0.1268 | No increase from 1.000 |
| 147/150 | 0.9778 | 0.0692 | 0.9583 | 0.1252 | No increase from 0.9722 |
| 148/150 | 0.9574 | 0.1291 | 0.9306 | 0.1992 | Increased |
| 149/150 | 0.9760 | 0.0827 | 0.9861 | 0.0412 | Increased |
| 150/150 | 0.9670 | 0.0932 | 0.9861 | 0.0502 | Same |

The system’s structure is presented in Table 5.

**Table 5: System Structure**

| Phase name | Dimensions (Result) | Parameters |
|---|---|---|
| ================================================================ | | |
| Convolution | (Nill, 200, 200, 32) | 2432 |

| | | |
|---|---|---|
| Convolution Iteration 1 | (Nill, 200, 200, 32) | 9248 |
| Maximum pooling | (Nill, 100, 100, 32) | 0 |
| Convolution Iteration 2 | (Nill, 100, 100, 64) | 18496 |
| Convolution Iteration 3 | (Nill, 100, 100, 64) | 36928 |
| Maximum pooling Iteration 1 | (Nill, 50, 50, 64) | 0 |
| Convolution Iteration 4 | (Nill, 50, 50, 128) | 73856 |
| Convolution Iteration 5 | (Nill, 50, 50, 128) | 147584 |
| Maximum pooling Iteration 2 | (Nill, 25, 25, 128) | 0 |
| Dropout | (Nill, 25, 25, 128) | 0 |
| Flattening | (Nill, 80000) | 0 |
| Dense | (Nill, 256) | 20480256 |
| Dropout Iteration 1 | (Nill, 256) | 0 |
| Dense Iteration 1 | (Nill, 128) | 32896 |
| Dropout Iteration 2 | (Nill, 128) | 0 |
| Dense Iteration 2 | (Nill, 6) | 774 |

=================================================================

Summation of parameters: 20,802,470
Learnable parameters: 20,802,470
Untrained parameters: 0

The pictures were labelled to represent these flaws as follows:

i. Pitted Surfaces (Ps): Pitting are surface irregularities. Pitted surfaces arise from localized corrosion which results in creation of holes in surfaces. Figure 2A: Sample A of Pitted Surfaces. Figure 2B – 2I: Succeeding images of Sample A taken at 20 degrees from the preceding image (AISI 1065 steel)

They are also sub-classified as a, b, c to i for the purpose of presentation. The images b to i represents the different orientations from which the images were taken. Images b to i were taken 20-degree inclination from its preceding image.

Figure 3A: Sample B of Pitted Surfaces. Figure 3B – 3I: Succeeding images of Sample B taken at 20 degrees from the preceding image (AISI 1065 steel).

Figure 4A: Sample C of Pitted Surfaces. Figure 4B – 4I: Succeeding images of Sample C taken at 20 degrees from the preceding image (AISI 1065 steel.

Figure A and Figure 5B – 5I: Succeeding images of Sample D taken at 20 degrees from the preceding image (AISI 1065 steel).

ii.Inclusions (In): inclusions occur when there is presence of materials (which may be non-metal) that are not wanted in the mix. They are shown in Figures: 6A-9A and 6B-9I.

iii.Rolled in Scales (Rs): these images were captured from surfaces that had scales and cracks as a result of rolling defects. Dataset for Rolled in Scales are captured. They are shown in Figures: 10A-13A and 10B-13I.

iv. Crazing (Cr): this occurs because of weakness of the metal in the crazed region. It is a visual crack and cannot be felt on the surfaces. They are similarly shown in Figures: 14A-17A and 17B-17I.

iv. Patches (Pa): patches are areas that differ from the microstructure of mix. This could be a result of welding a piece of metal to a blank. They are presented in Figures: 18A-21A and 21B-21I.

vi. Scratches (Sc): scratches occur mostly as a result of abrasion particles which impact the surface of metals. The dataset for Scratches are presented in Figures: 22A-25A and 22B-25I.

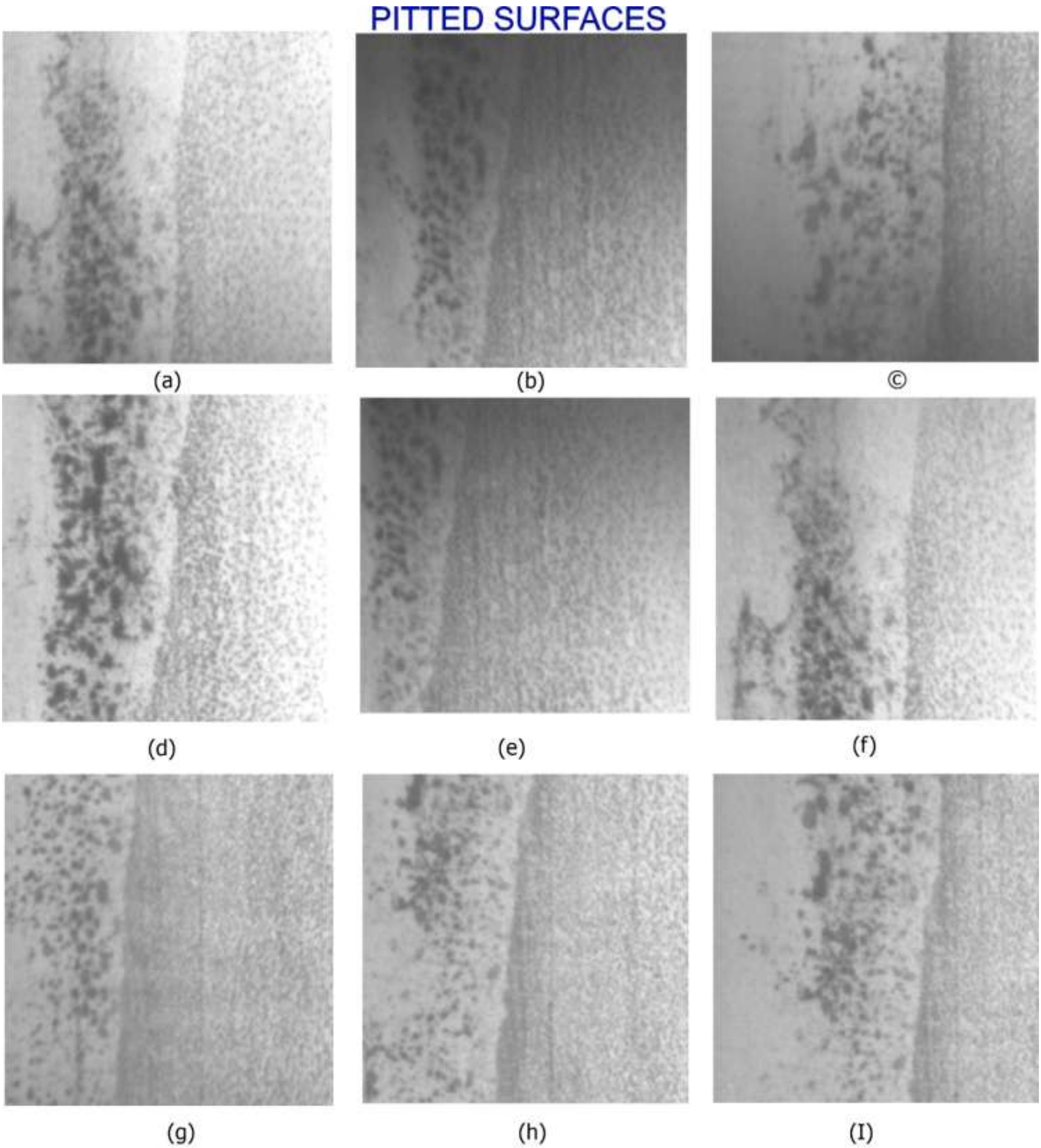


**Figure 2A: Sample A of Pitted Surfaces. Figure 2B – 2I: Succeeding images of Sample A taken at 20 degree from the preceding image (AISI 1065 steel)**

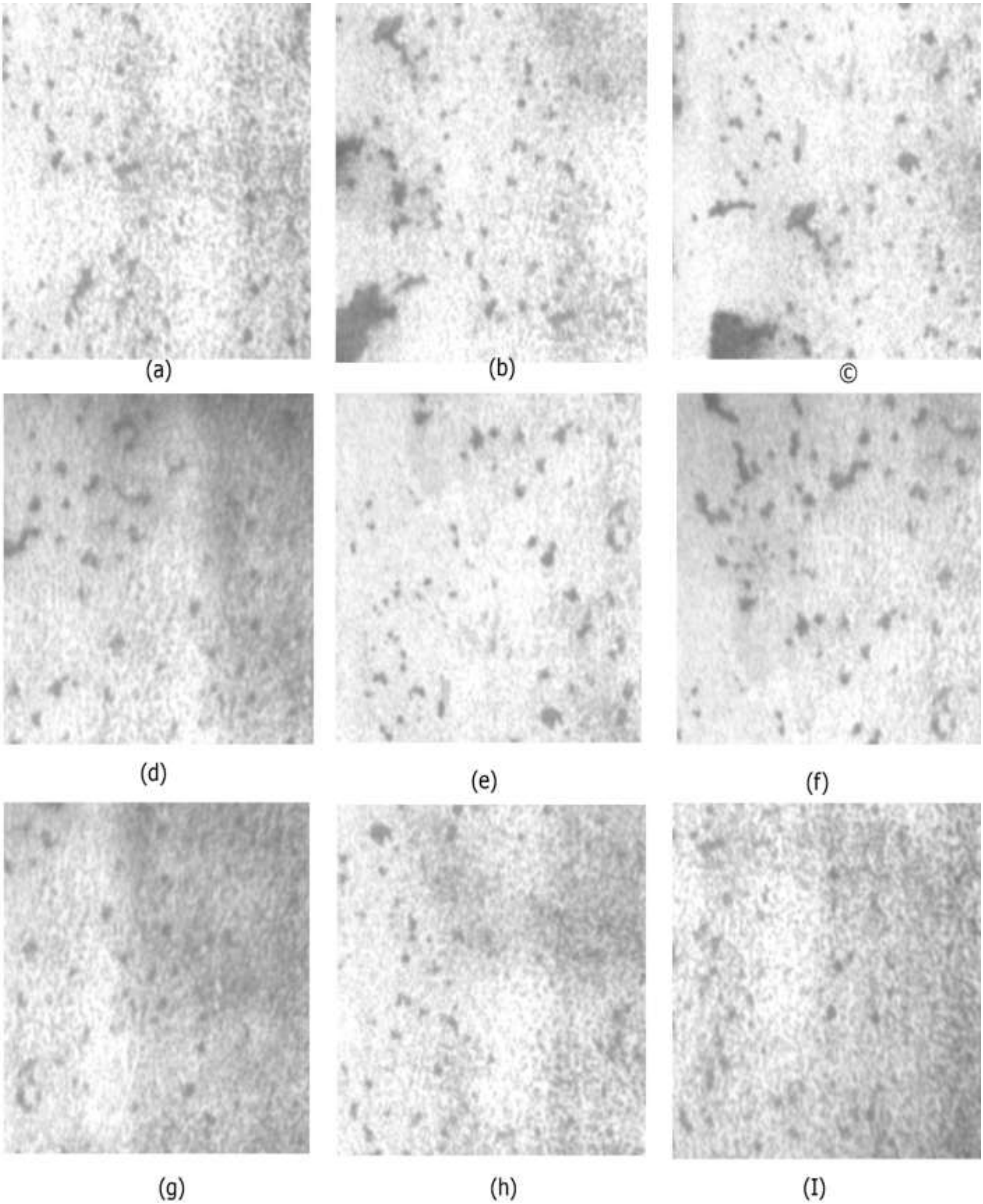


**Figure 3A: Sample B of Pitted Surfaces. Figure 3B – 3I: Succeeding images of Sample B taken at 20 degree from the preceding image (AISI 1065 steel)**

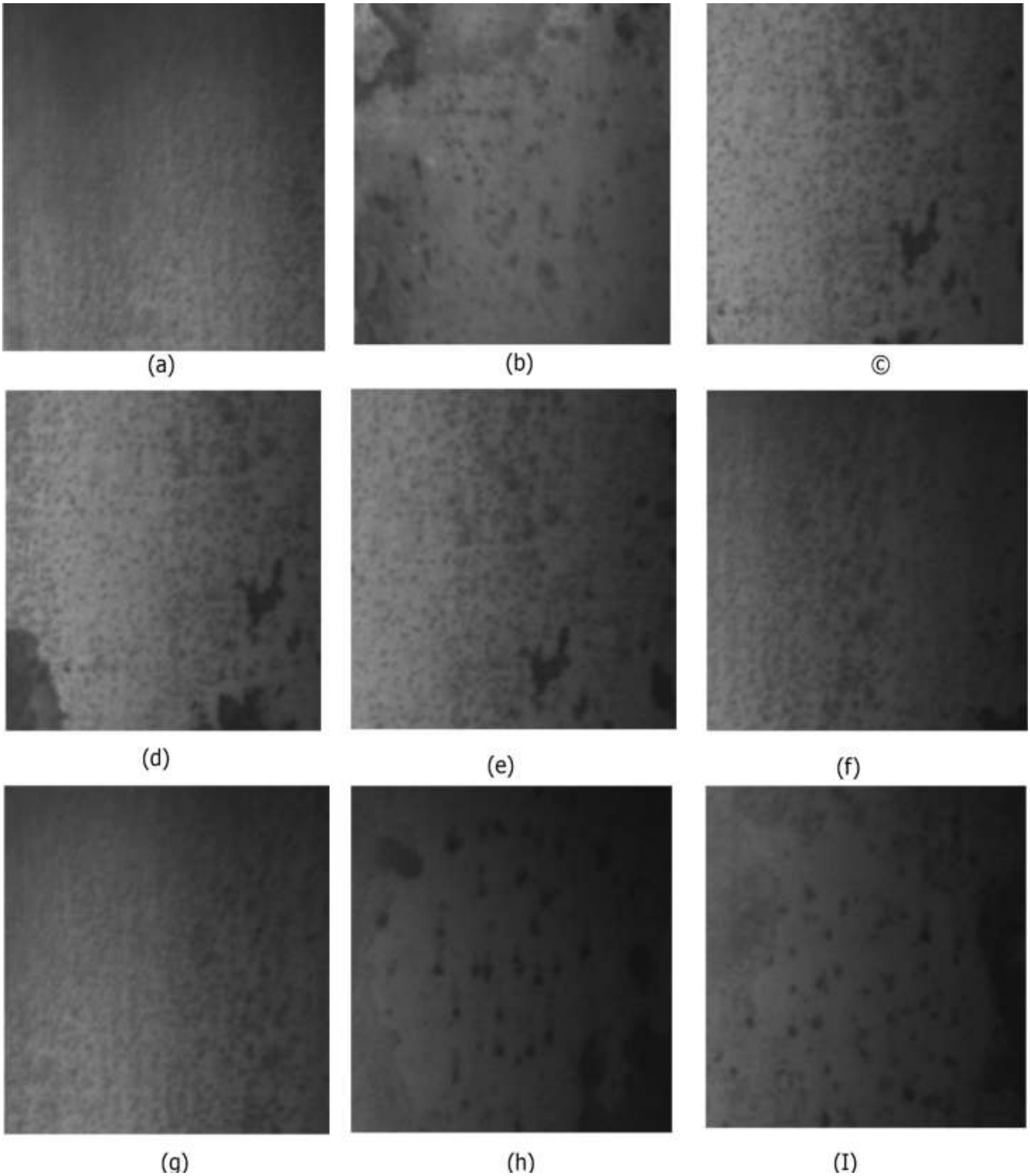


**Figure 4A: Sample C of Pitted Surfaces. Figure 4B – 4I: Succeeding images of Sample C taken at 20 degree from the preceding image (AISI 1065 steel)**

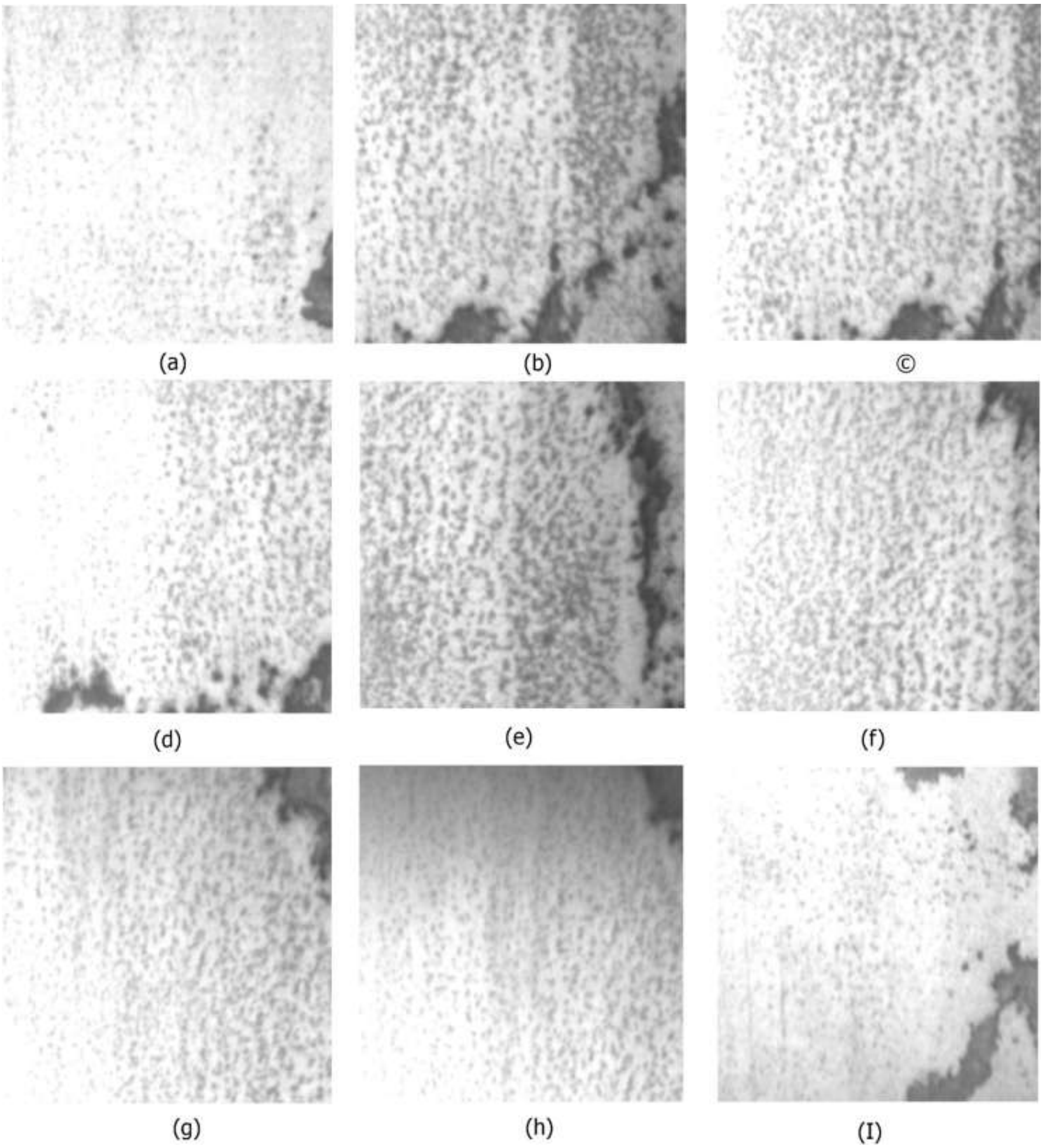


**Figure 5A: Sample D of Pitted Surface. Figure 5B – 5I: Succeeding images of Sample D taken at 20 degree from the preceding image (AISI 1065 steel)**

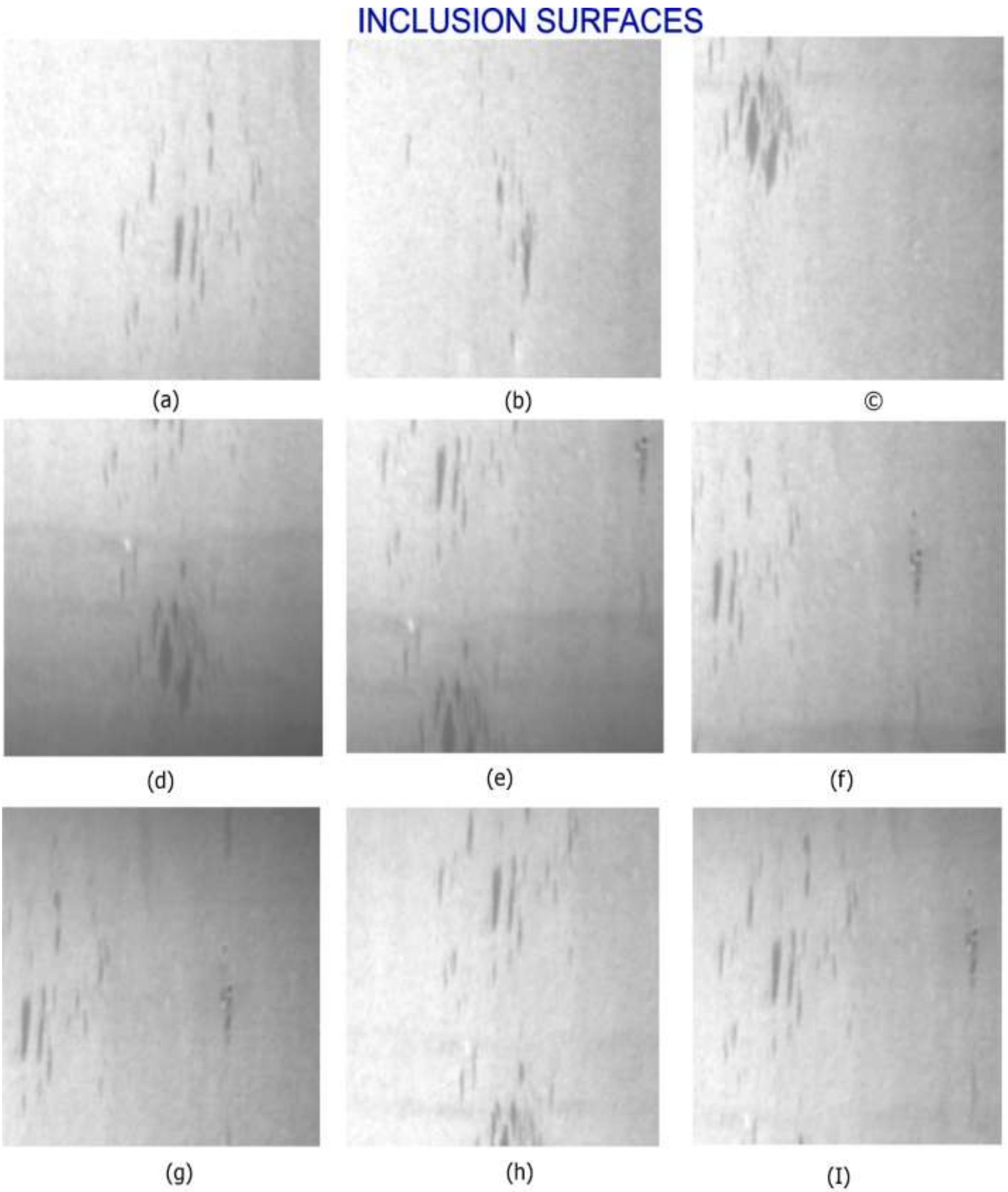


**Figure 6A: Sample A of Inclusion Surface. Figure 6B – 6I: Succeeding images of Sample D taken at 20 degree from the preceding image (AISI 1065 steel)**

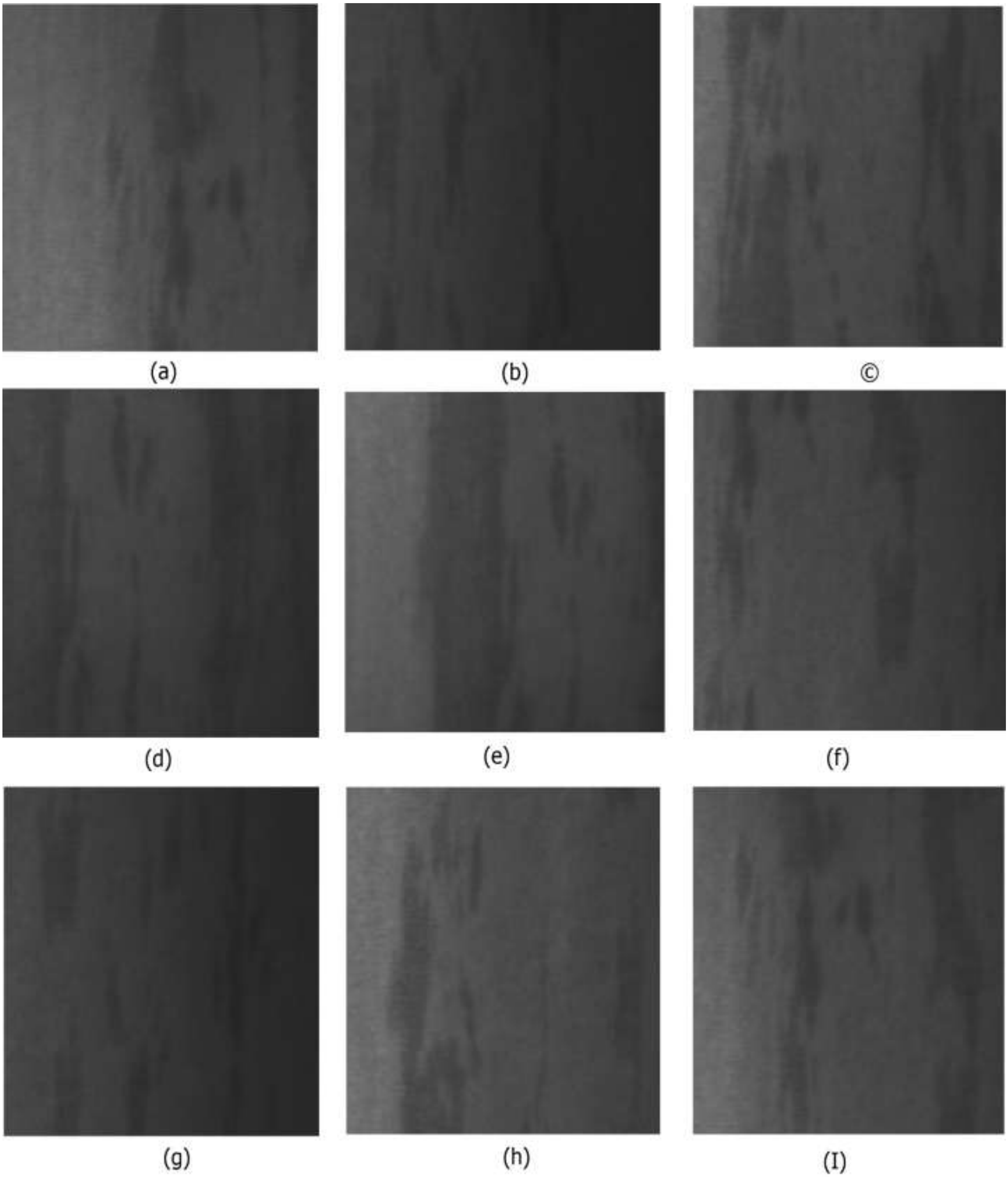


**Figure 7A: Sample B of Inclusion Surface. Figure 7B – 7I: Succeeding images of Sample D taken at 20 degree from the preceding image (AISI 1065 steel)**

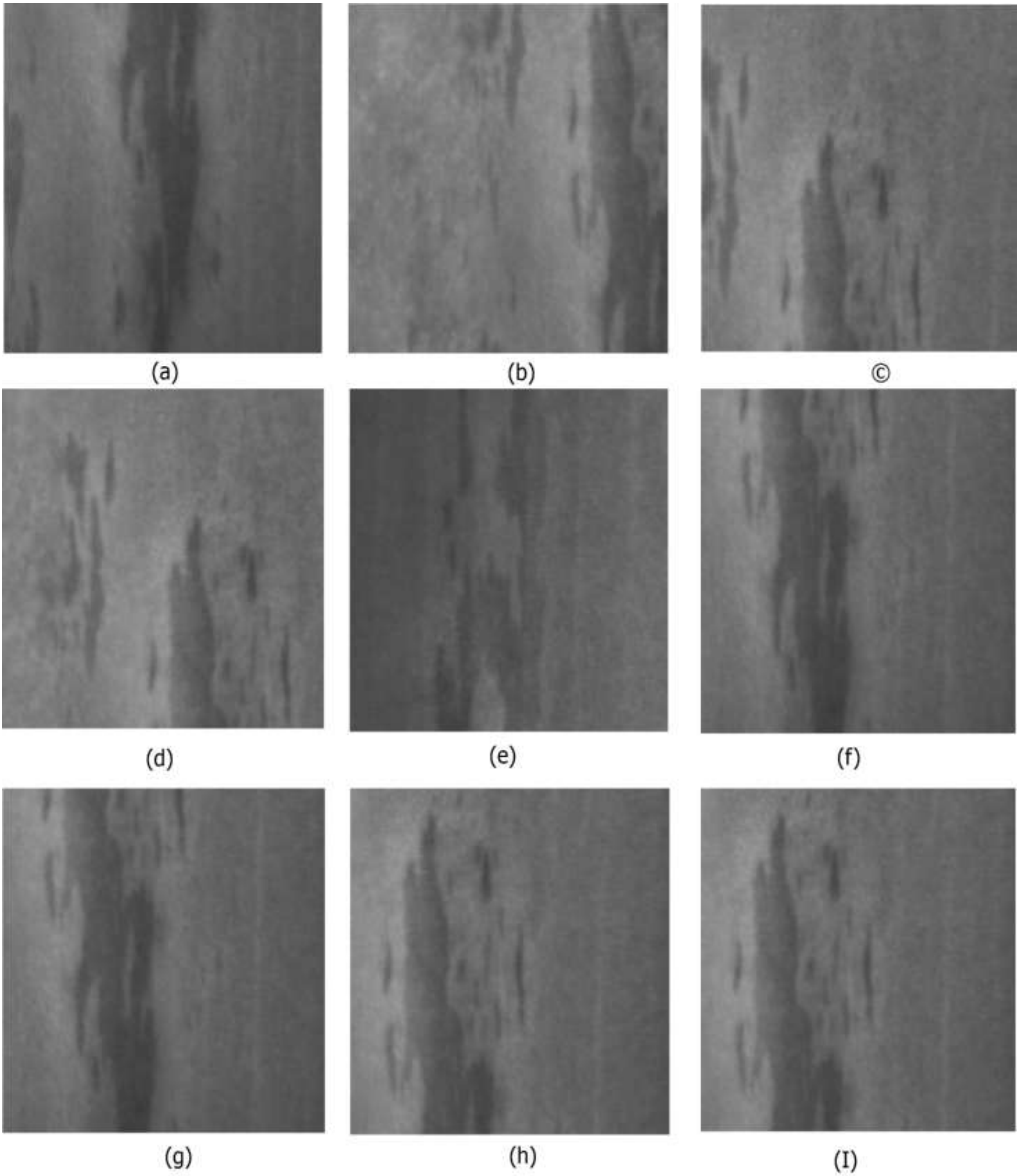


**Figure 8A: Sample C of Inclusion Surface. Figure 8B – 8I: Succeeding images of Sample C taken at 20 degree from the preceding image (AISI 1065 steel)**

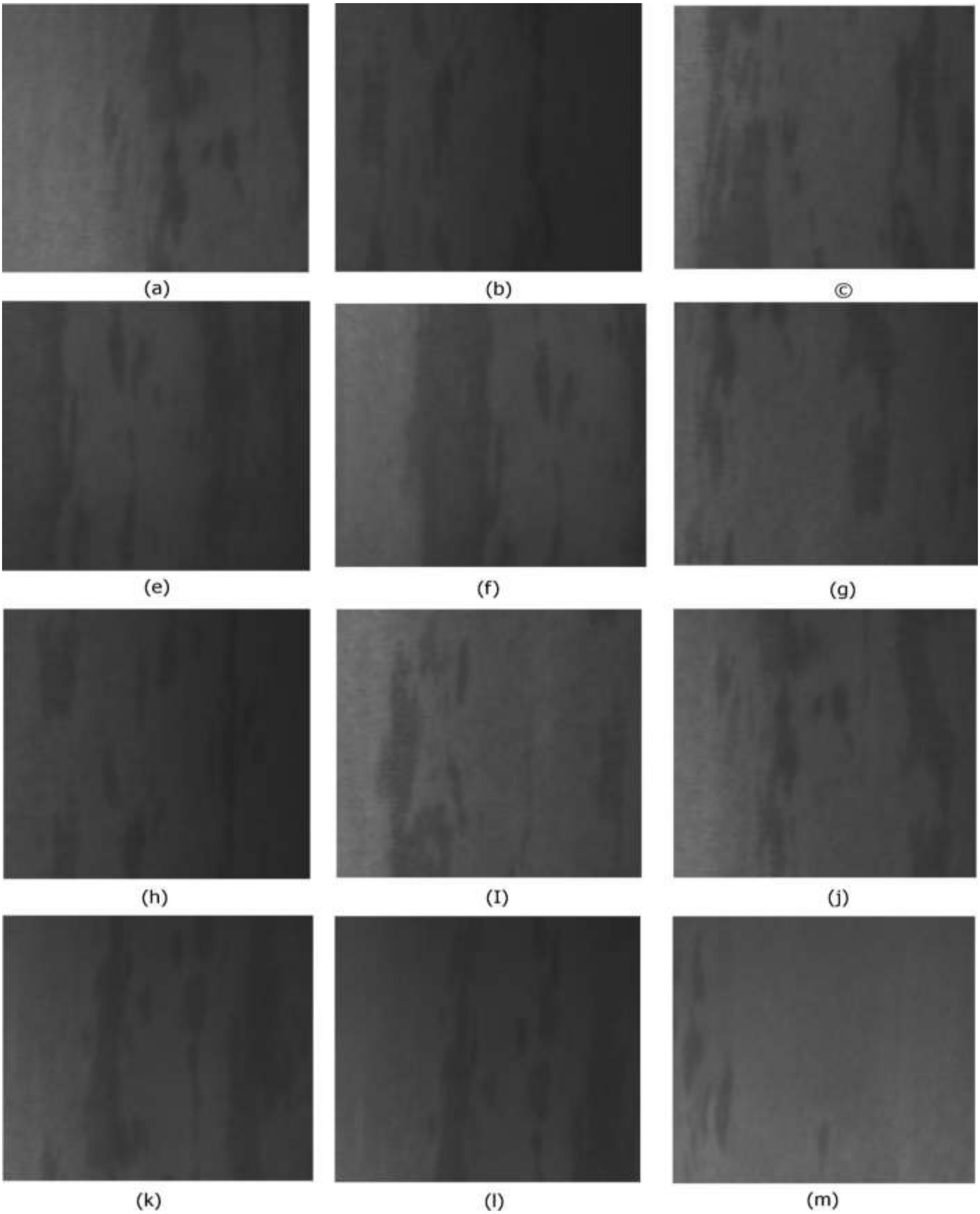


**Figure 9A: Sample D of Inclusion Surface. Figure 9B -9I: Succeeding images of Sample D taken at 20 degree from the preceding image (AISI 1065 steel)**

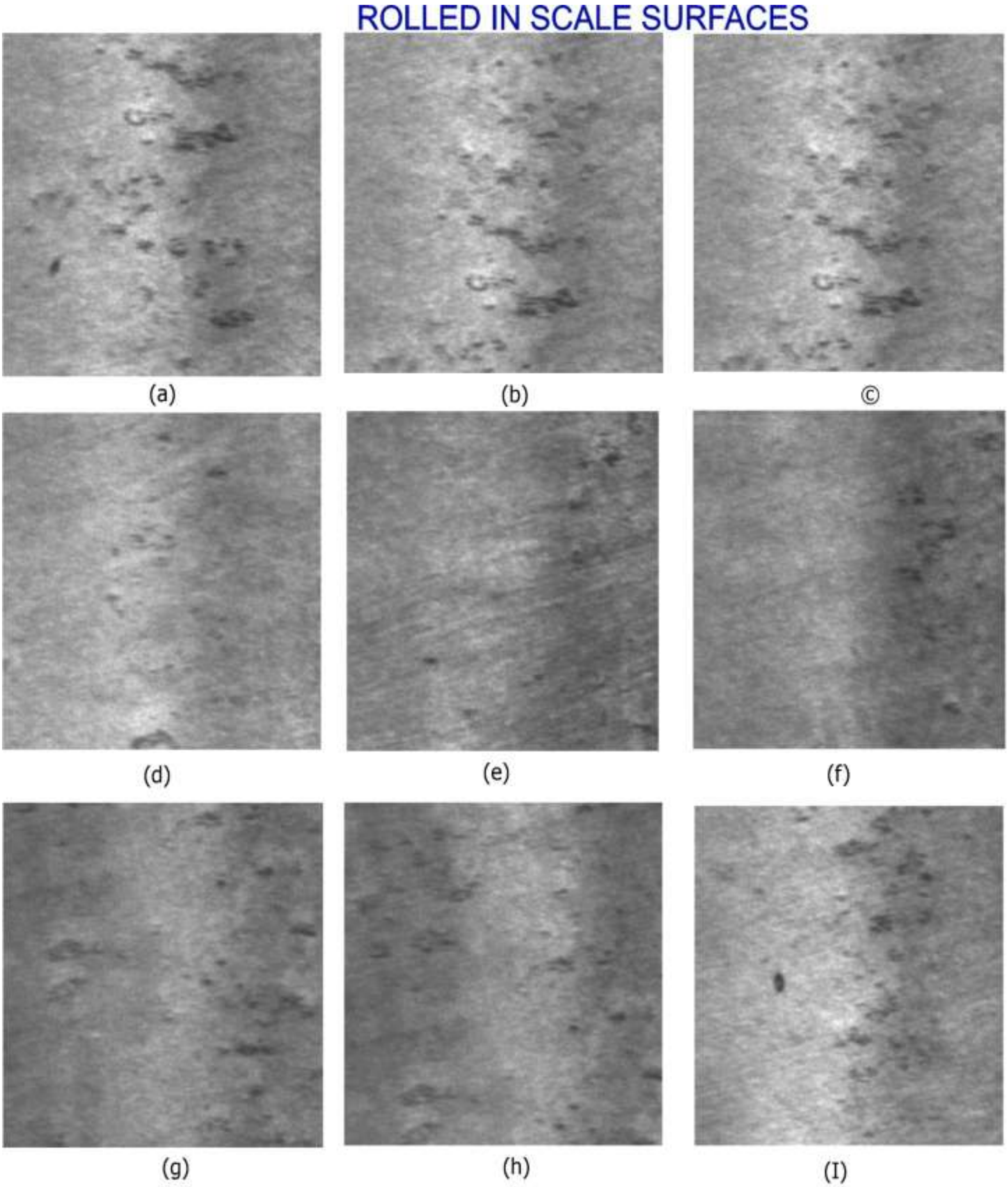


**Figure 10A: Sample A of Rolled in Scale Surface. Figure 10B – 10I: Succeeding images of Sample A taken at 20 degree from the preceding image (AISI 1065 steel)**

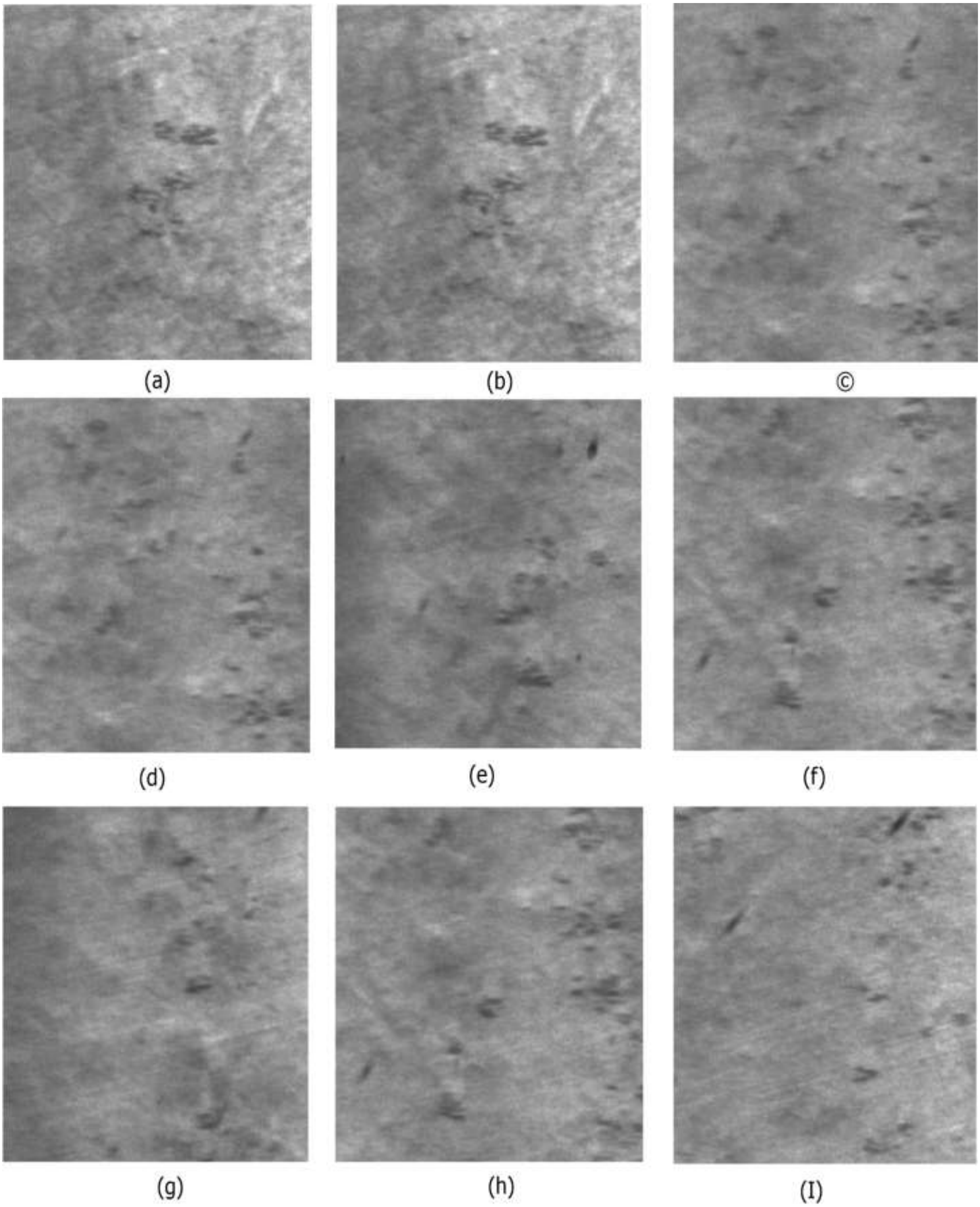


**Figure 11A: Sample B of Rolled in Scale Surface. Figure 11B – 11I: Succeeding images of Sample B taken at 20 degree from the preceding image (AISI 1065 steel)**

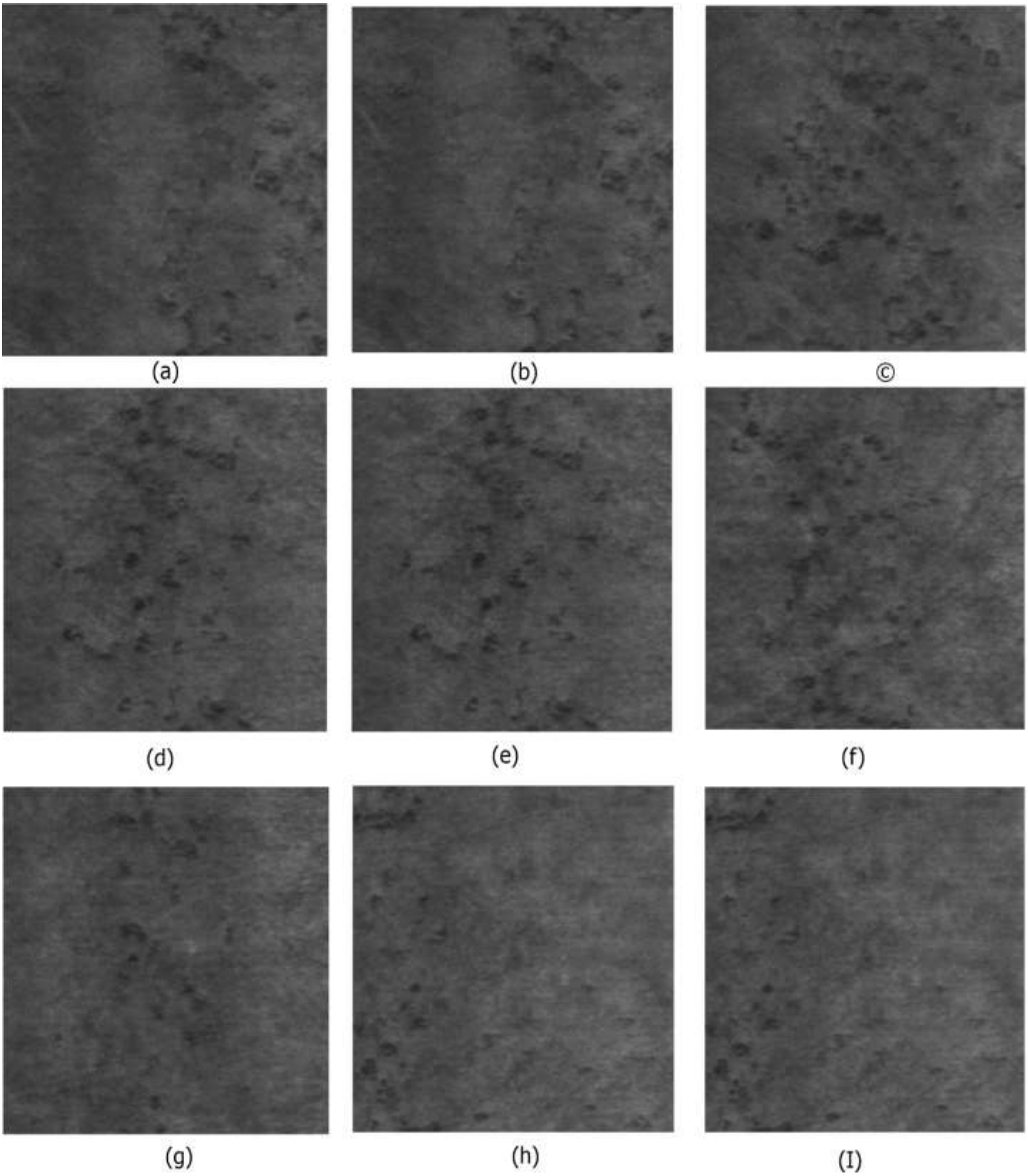


**Figure 12A: Sample C of Rolled in Scale Surface. Figure 12B – 12I: Succeeding images of Sample C taken at 20 degree from the preceding image (AISI 1065 steel)**

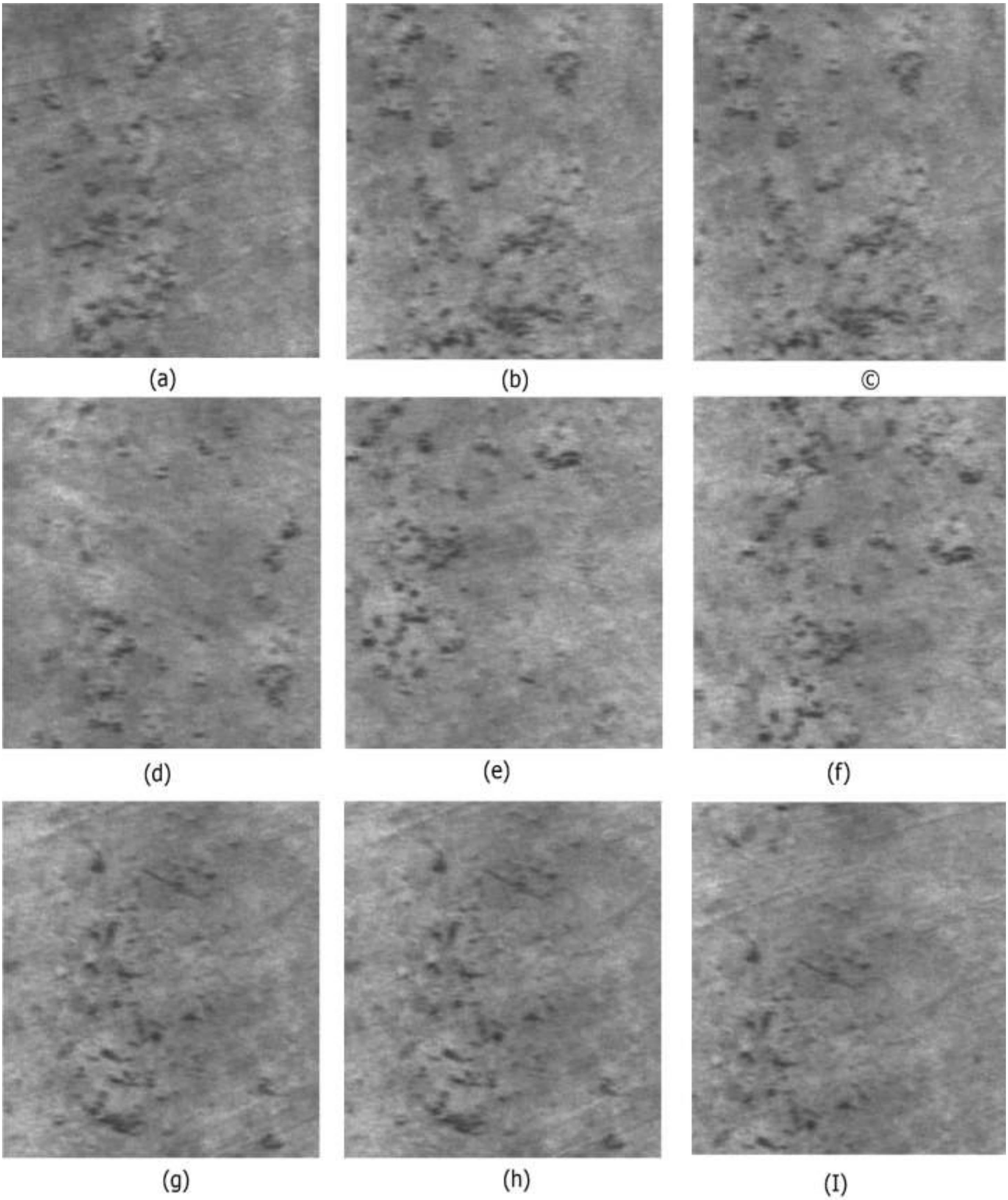


**Figure 13A: Sample D of Rolled in Scale Surface. Figure 13B – 13C: Succeeding images of Sample D taken at 20 degree from the preceding image (AISI 1065 steel)**

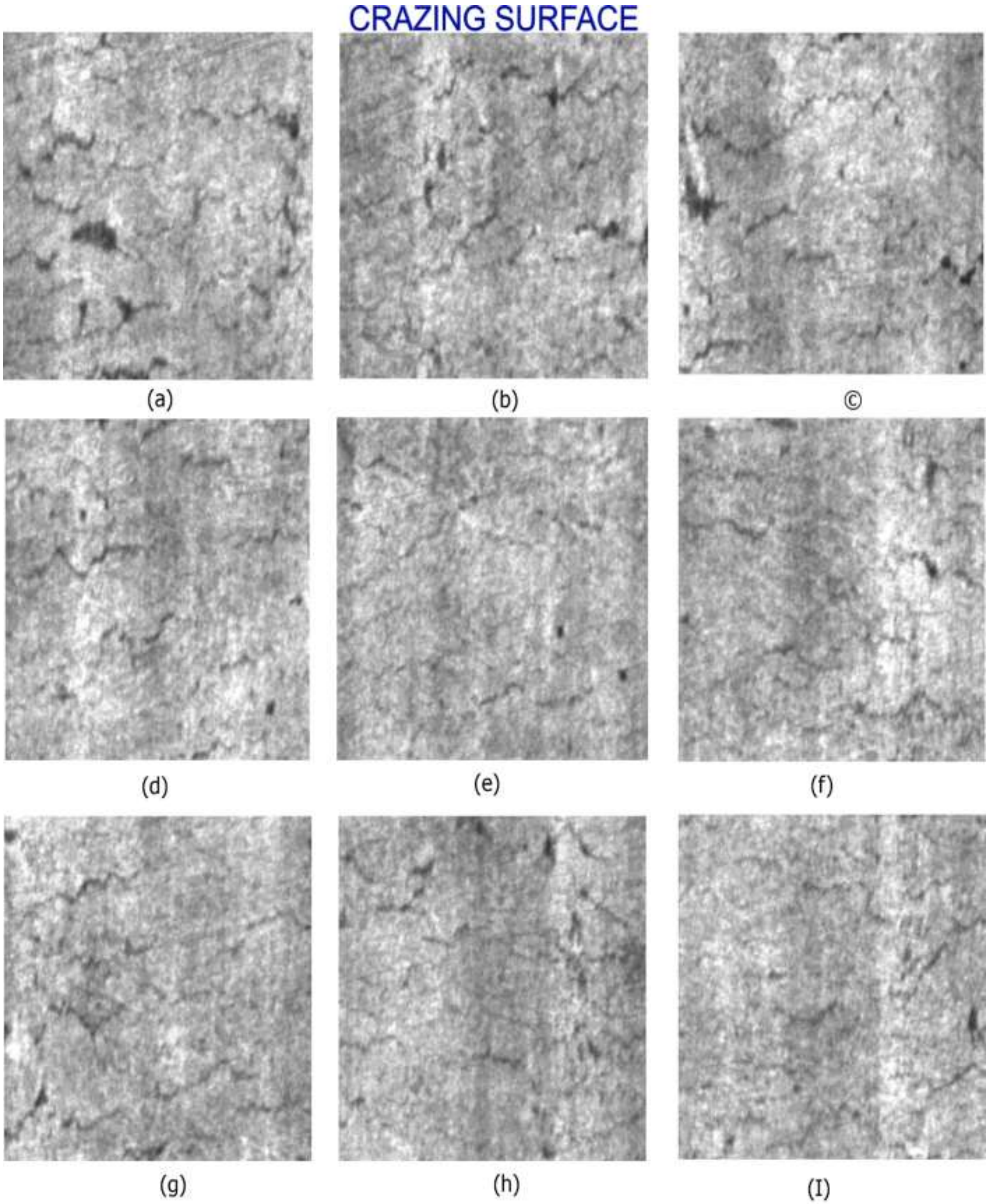


**Figure 14A: Sample A of Crazing Surface. Figure 14B – 14I: Succeeding images of Sample A taken at 20 degree from the preceding image (AISI 1065 steel)**

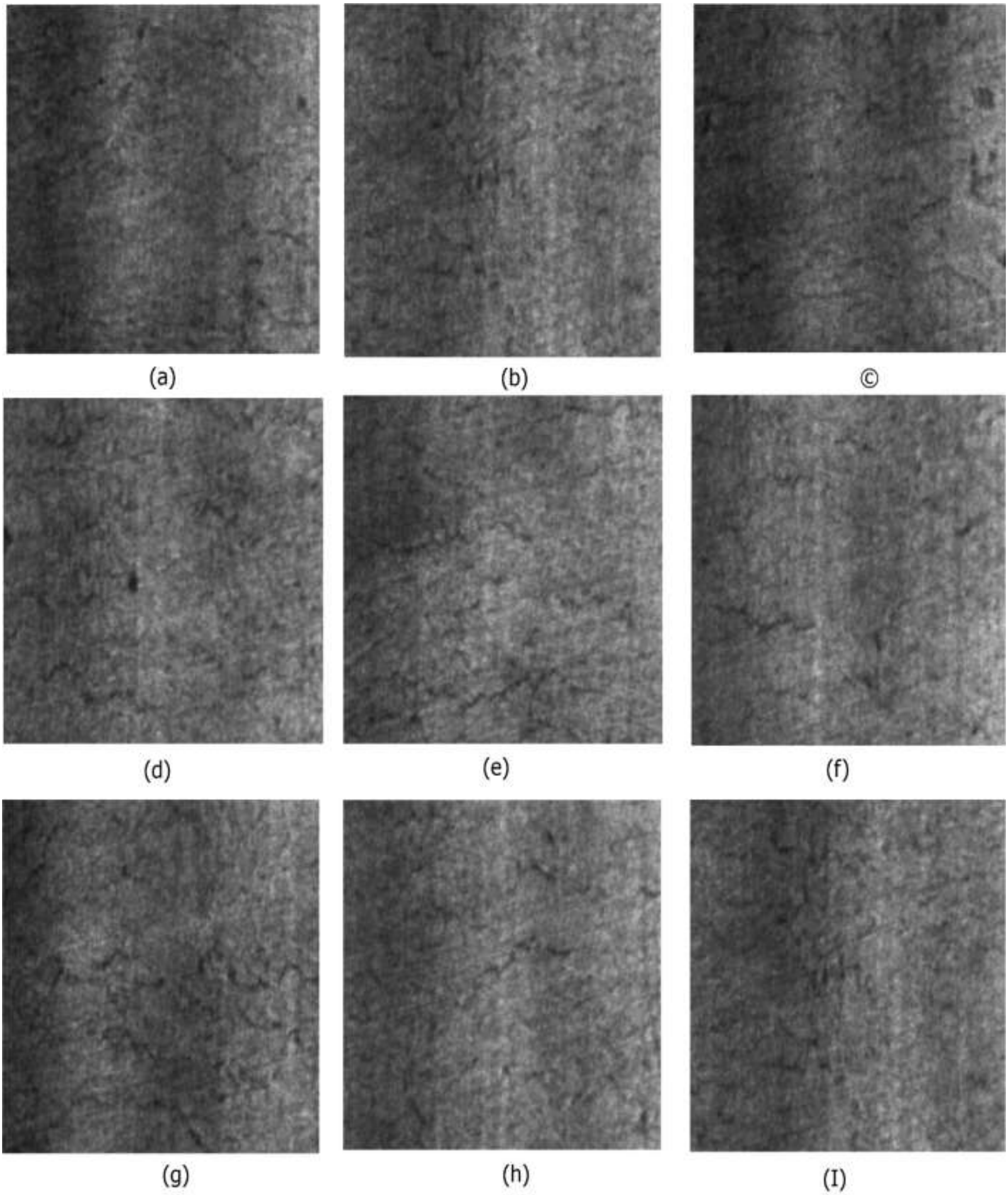


**Figure 15A: Sample B of Crazing Surface. Figure 15B - 15I: Succeeding images of Sample B taken at 20 degree from the preceding image (AISI 1065 steel)**

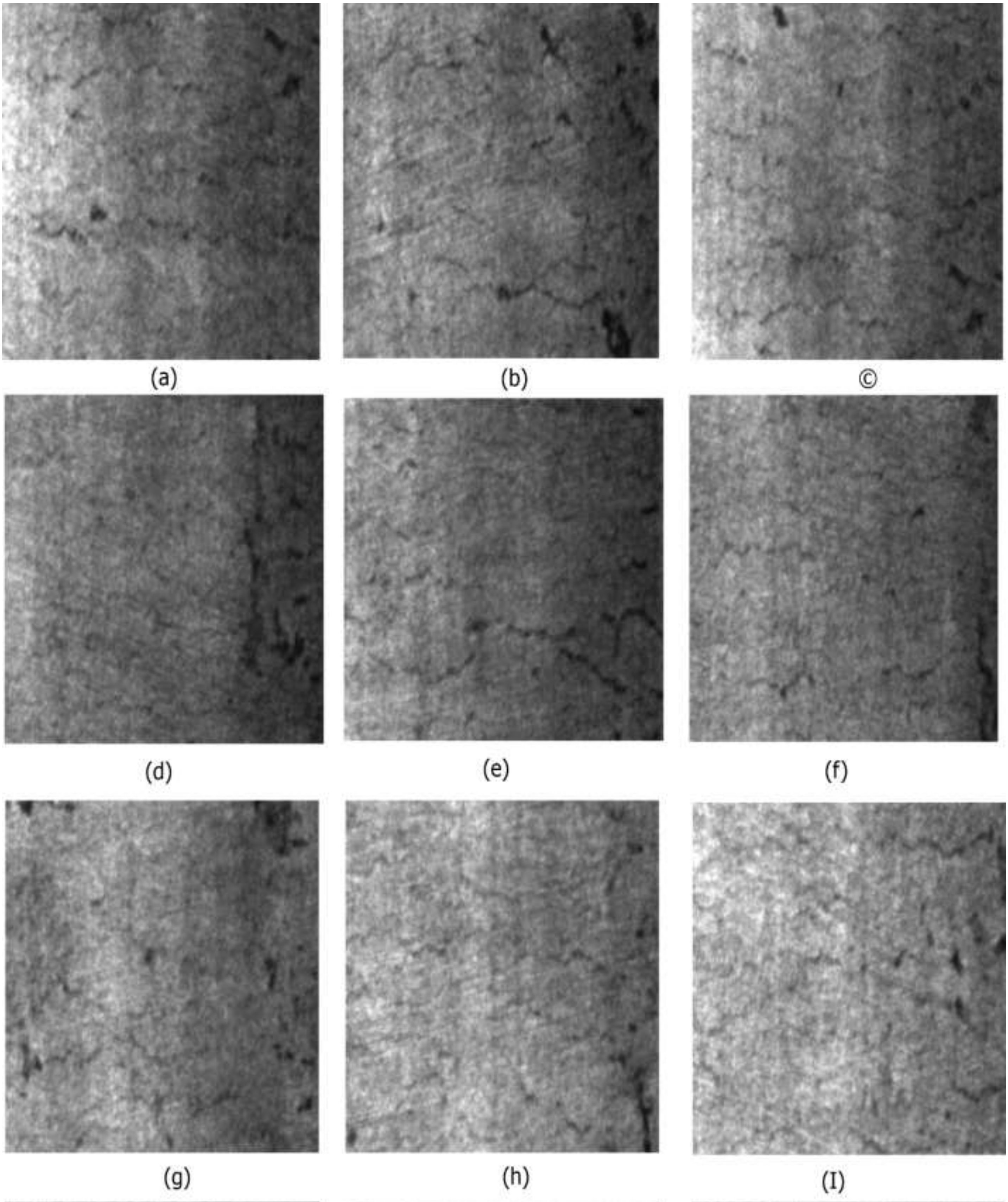


**Figure 16A: Sample C of Crazing Surface. Figure 16B – 16I: Succeeding images of Sample C taken at 20 degree from the preceding image (AISI 1065 steel)**

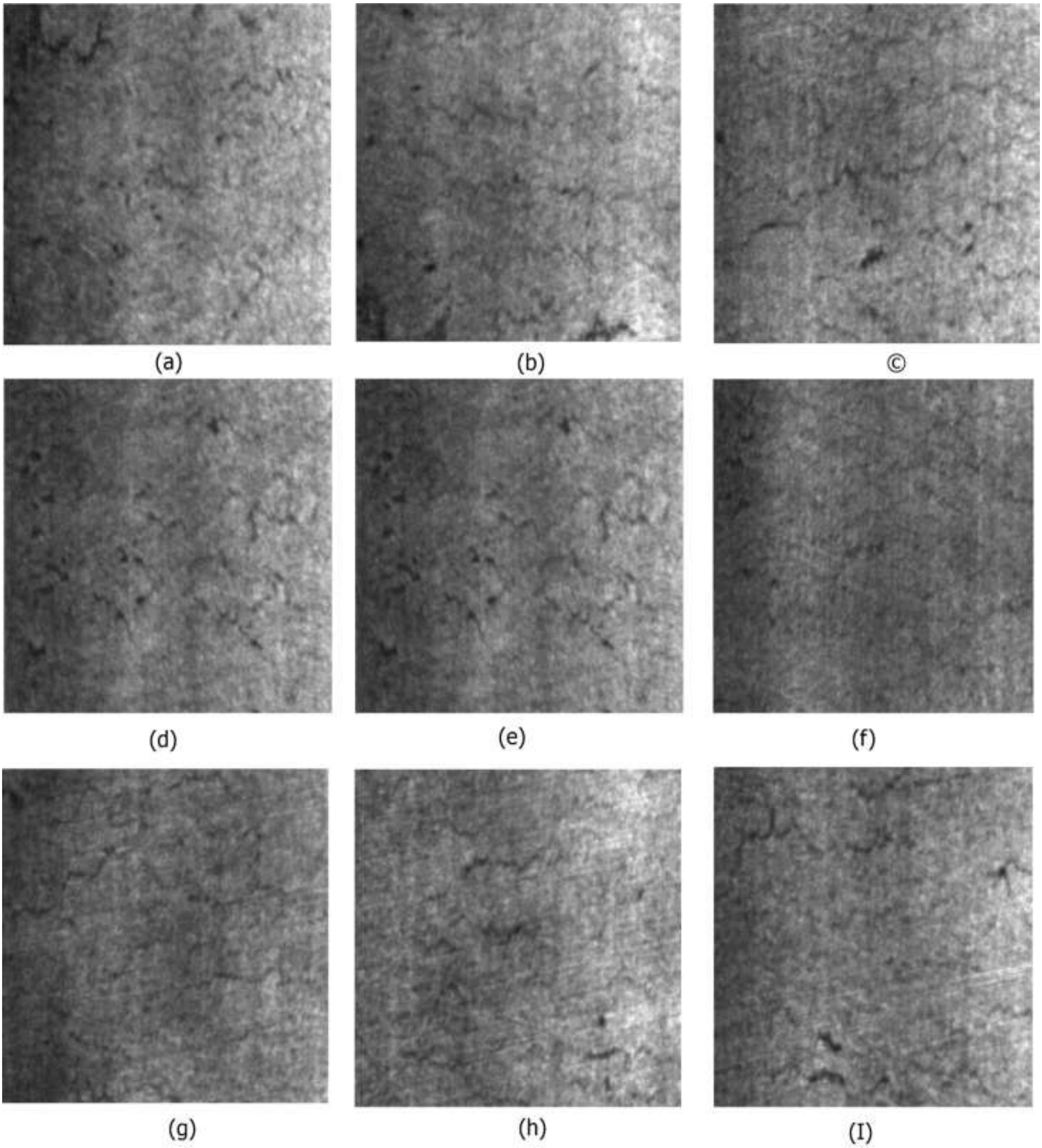


**Figure 17A: Sample D of Crazing Surface. Figure 17B -17I: Succeeding images of Sample D taken at 20 degree from the preceding image (AISI 1065 steel)**

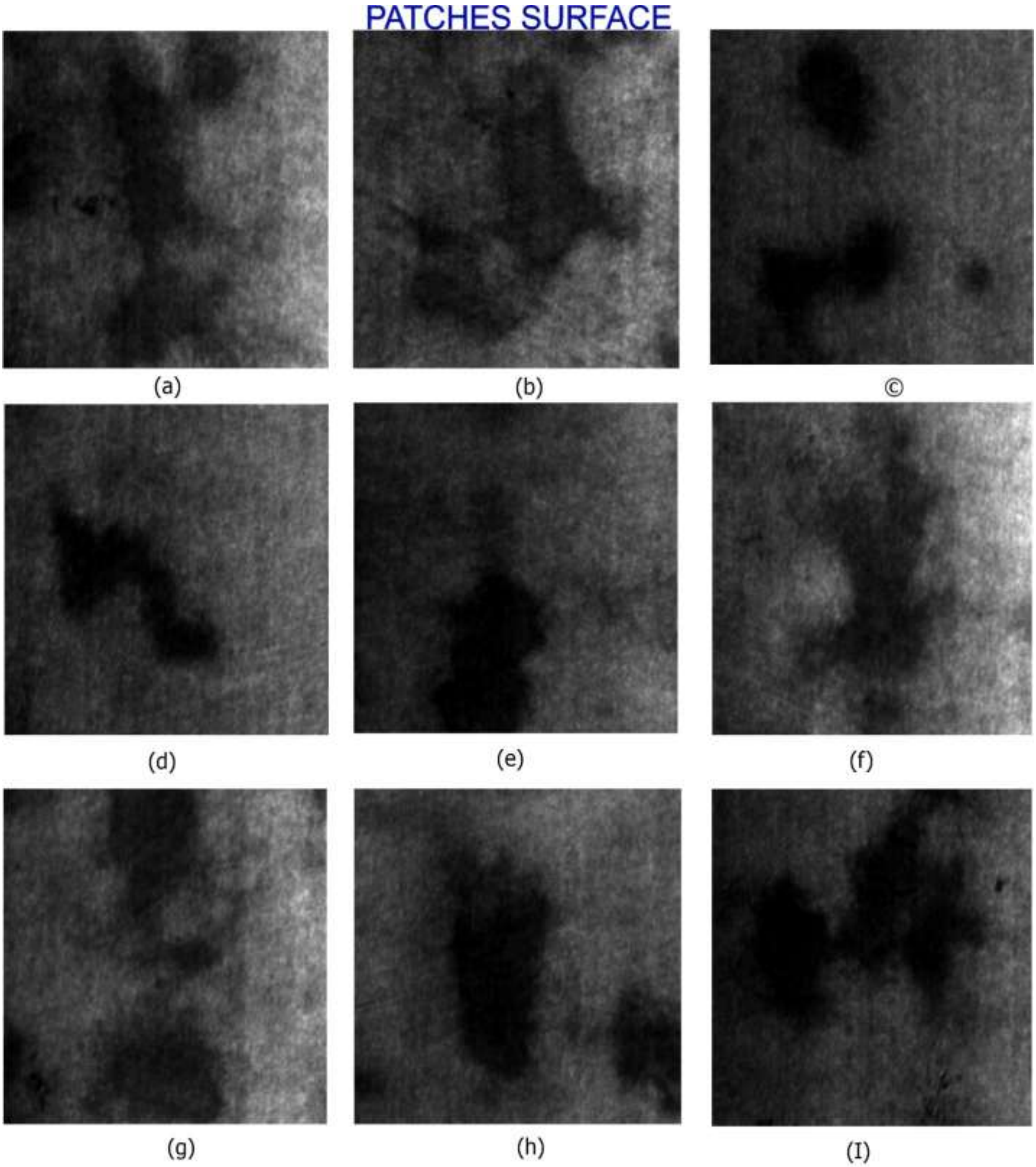


**Figure 18A: Sample A of Patch Surface. Figure 18B – 18I: Succeeding images of Sample A taken at 20 degrees from the preceding image (AISI 1065 steel)**

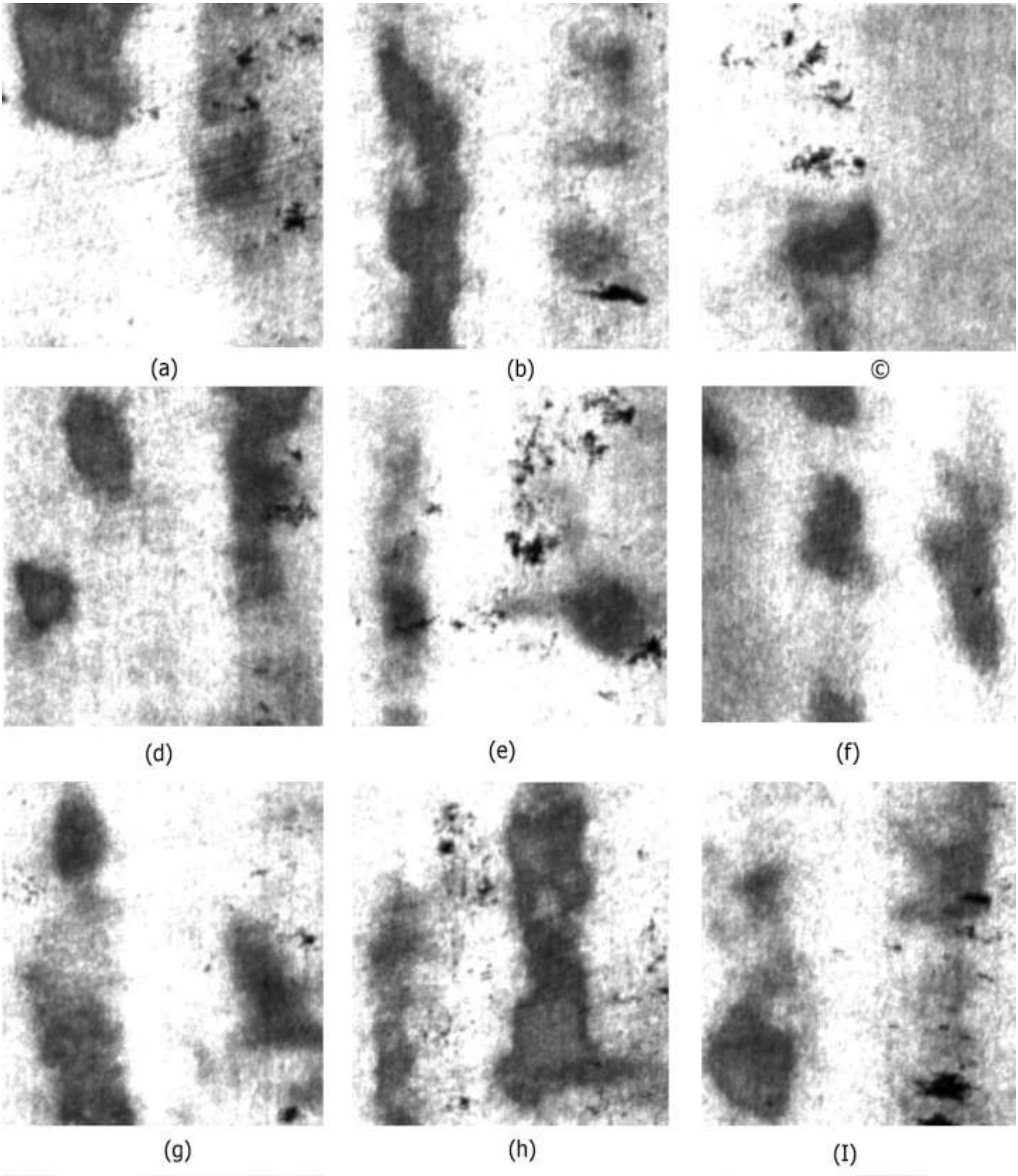


**Figure 19A: Sample B of Patch Surface. Figure 19B-19I: Succeedng images of Sample B taken at 20 degree from the preceding image (AISI 1065 steel)**

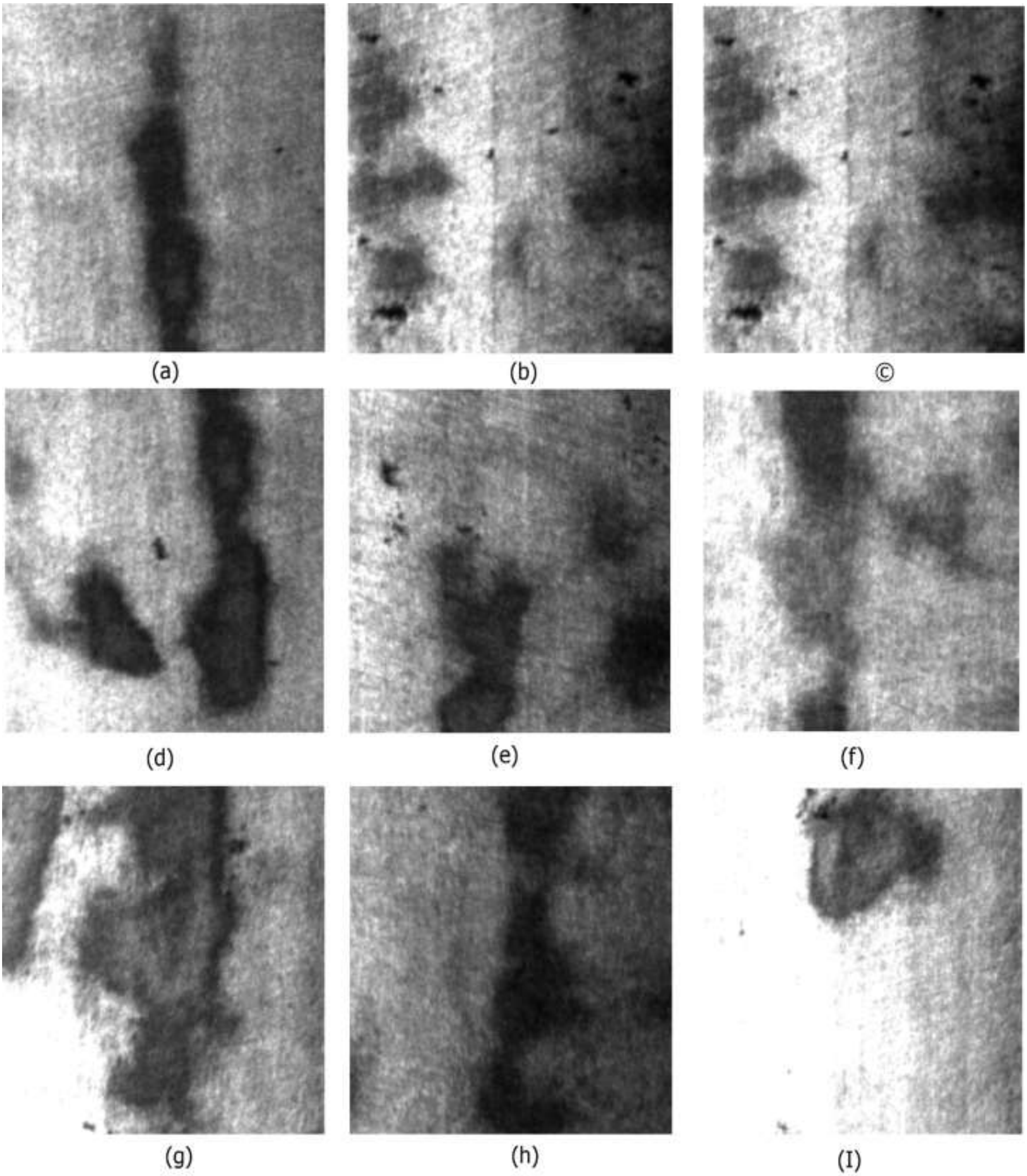

Figure 20A: Sample C of Patch Surface. Figure 20B – 20I: Succeding images of Sample C taken at 20 degree from the preceding image (AISI 1065 steel)

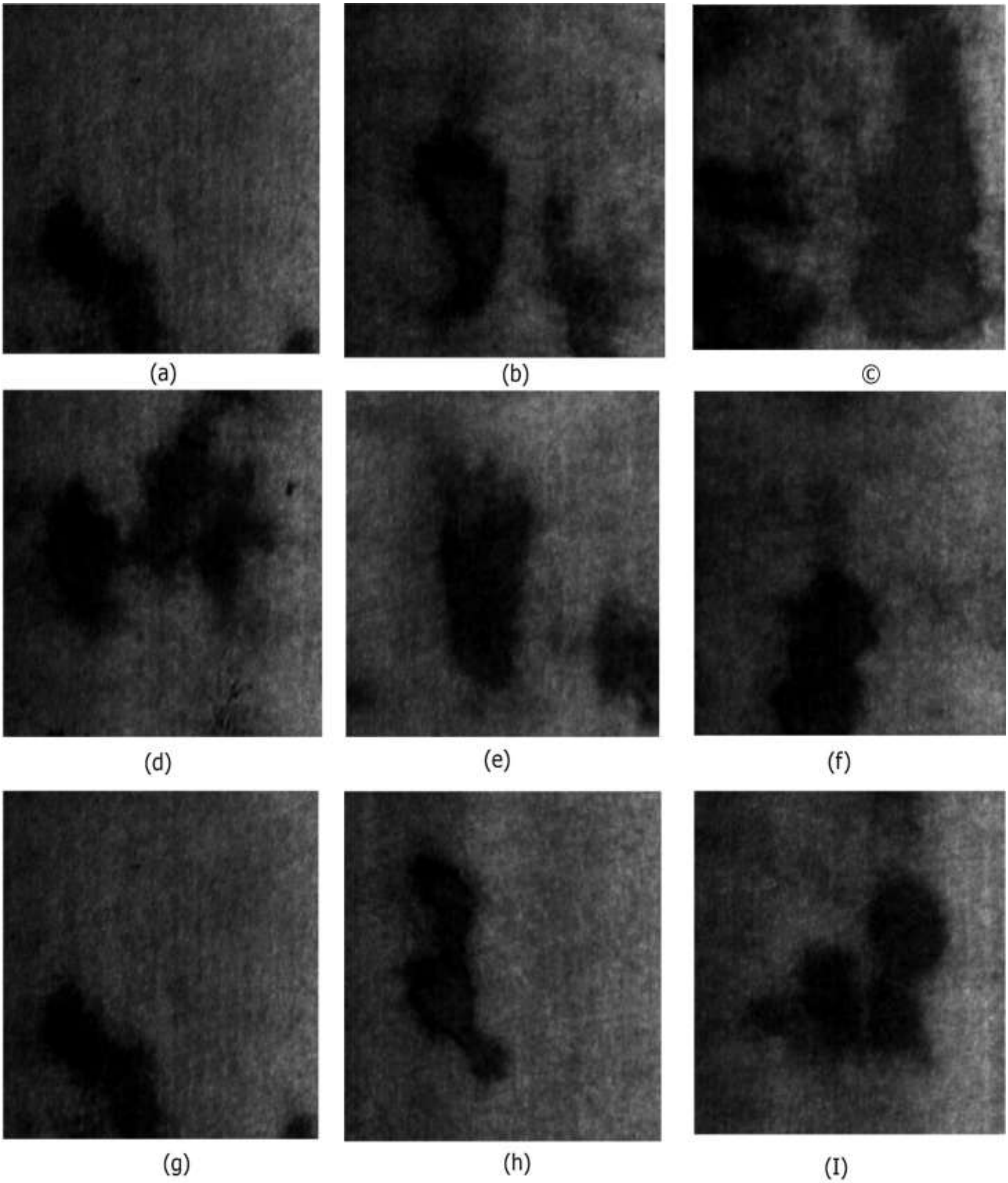


**Figure 21A: Sample D of Patch Surface. Figure 21B – 21I: Succeeding images of Sample D taken at 20 degree from the preceding image (AISI 1065 steel)**

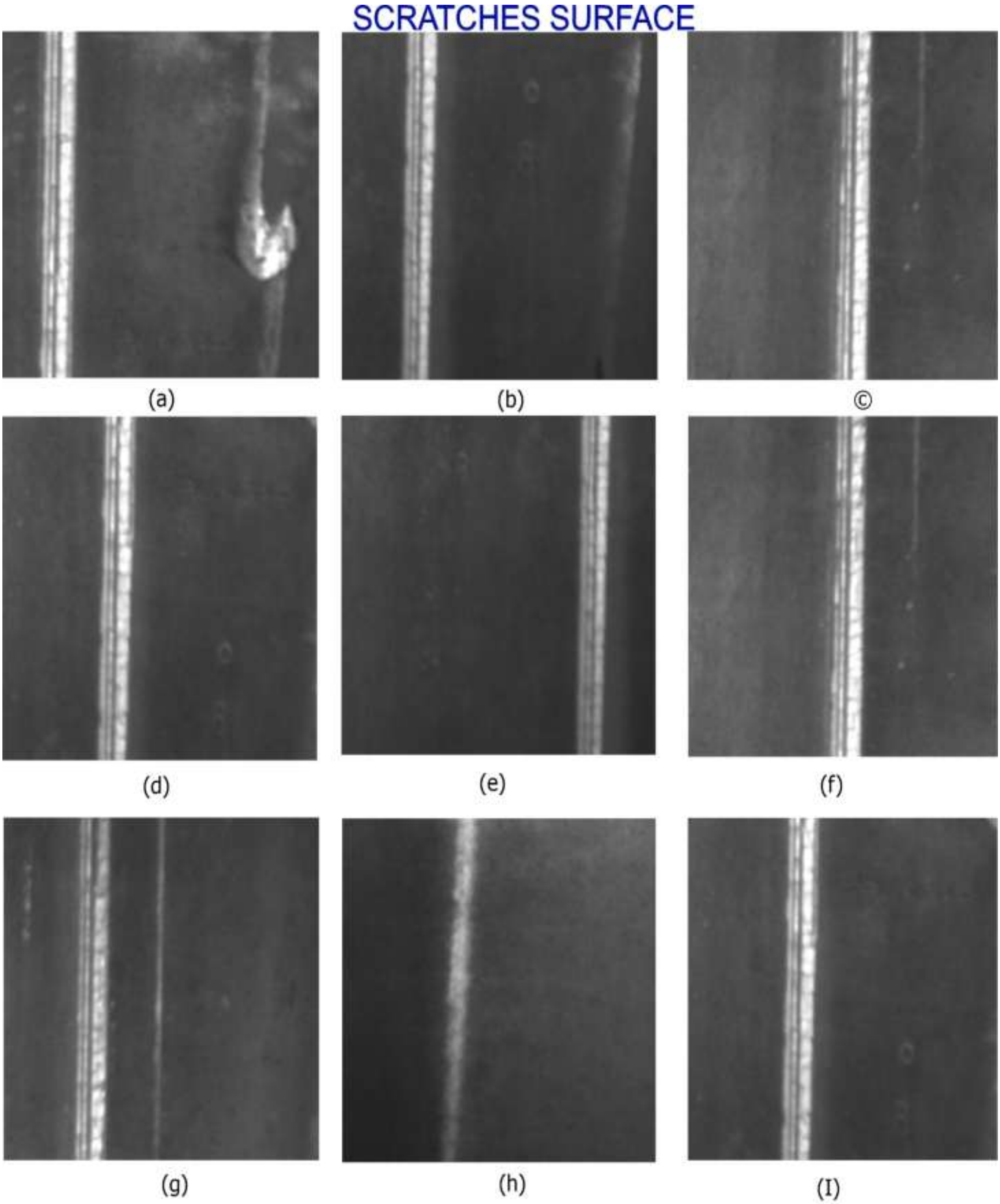


**Figure 22A: Sample A of Scratch Surface. Figure 22B – 22I: Succeeding images of Sample A taken at 20 degree from the preceding image (AISI 1065 steel)**

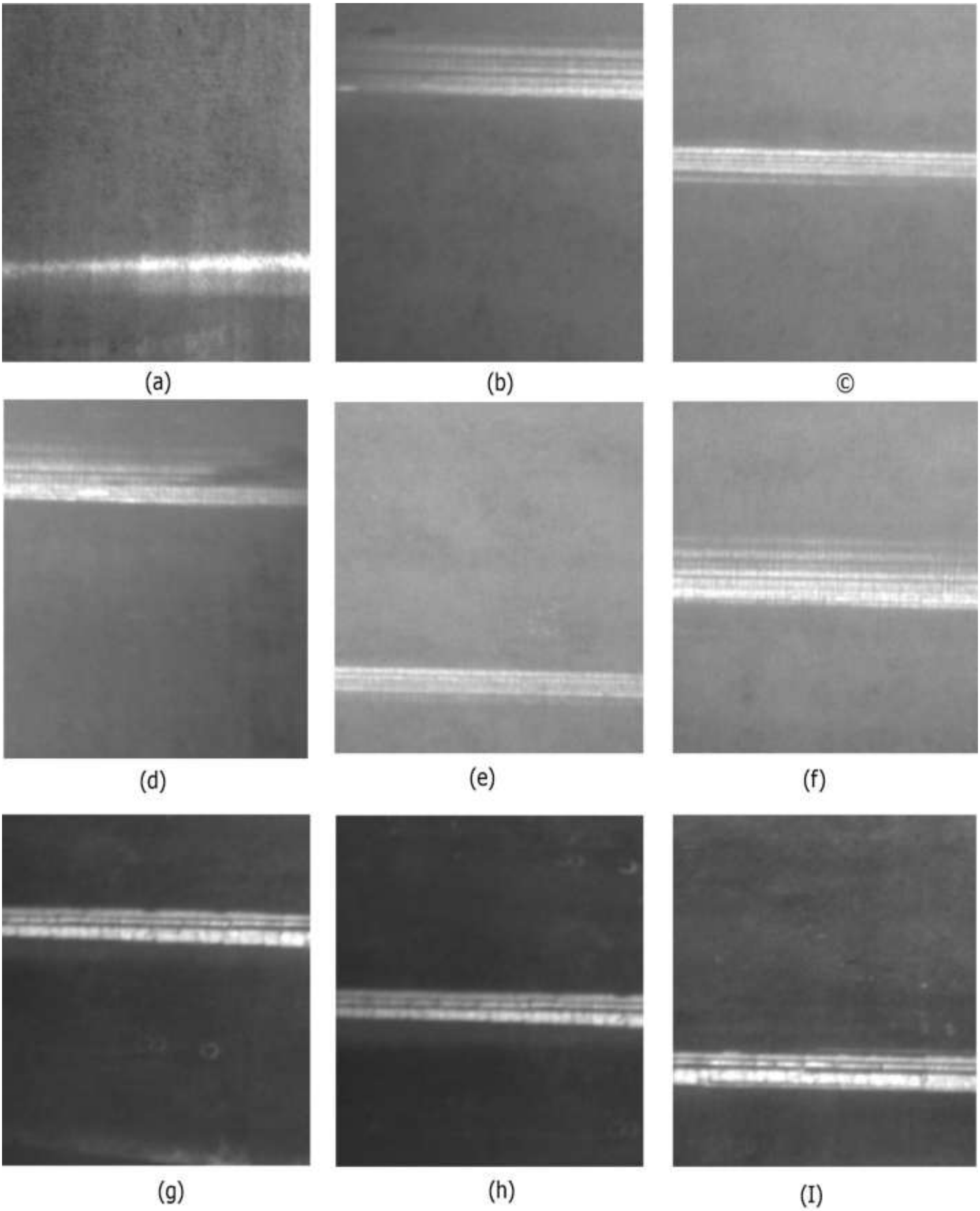


**Figure 23A: Sample B of Scratch Surface. Figure 23B – 23I: Succeeding images of Sample B taken at 20 degree from the preceding image (AISI 1065 steel)**

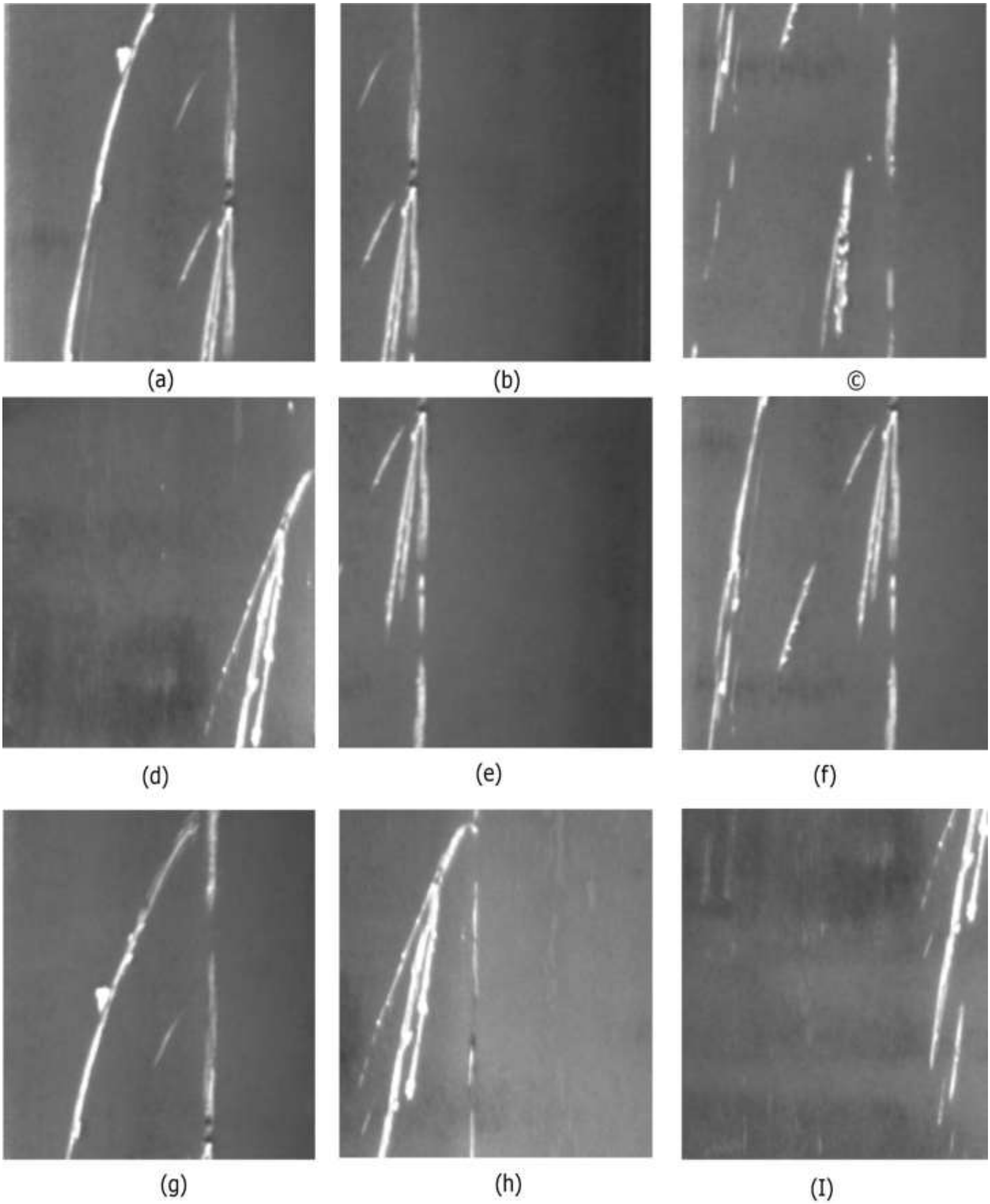


**Figure 24A: Sample C of Scratch Surface. Figure 24B – 24I: Succeeding images of Sample C taken at 20 degree from the preceding image (AISI 1065 steel)**

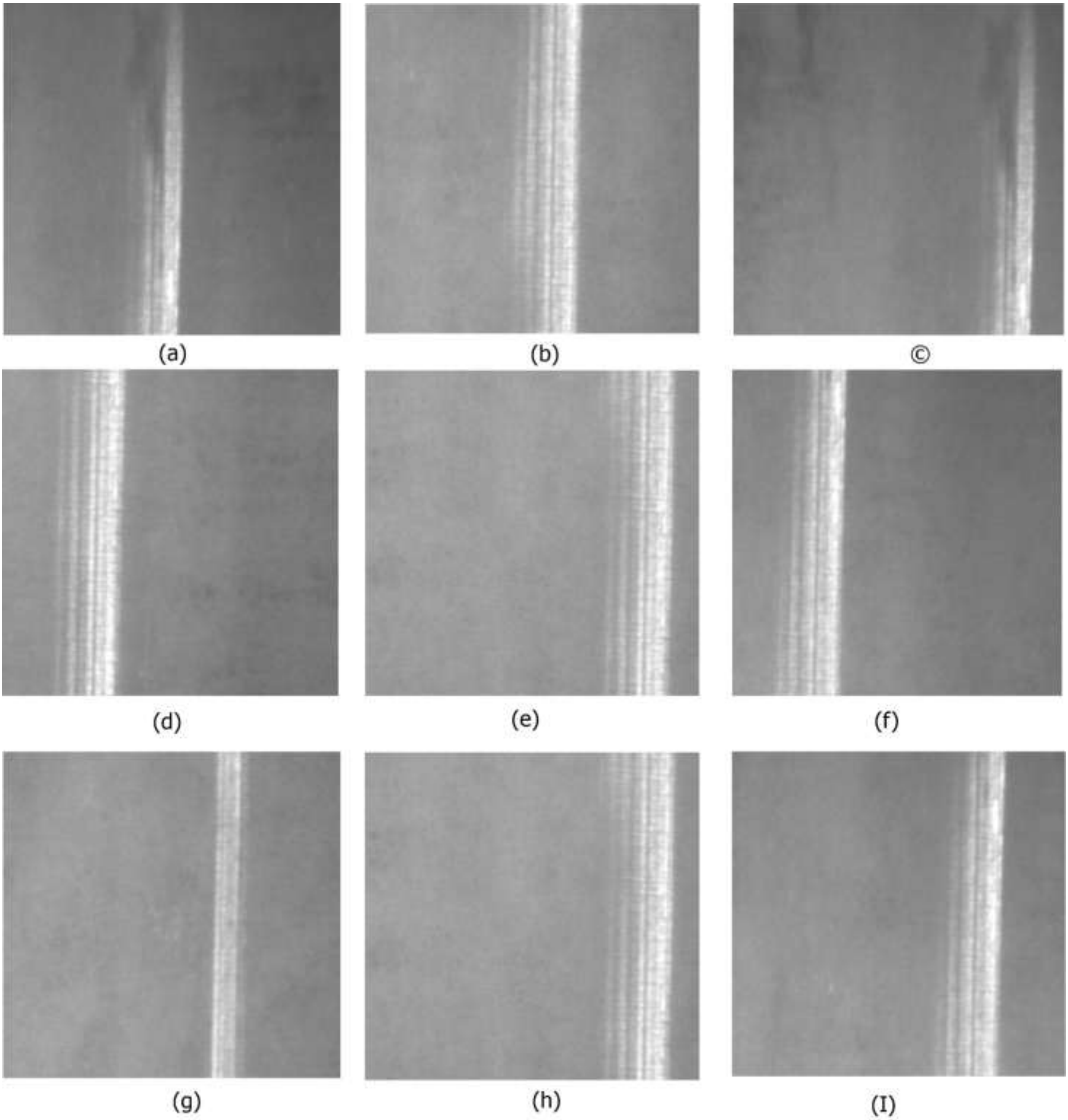

**Figure 25A: Sample D of Scratch Surface. Figure 25B – 25I: Succeeding images of Sample D taken at 20 degree from the preceding image (AISI 1065 steel)**

**Table 7: Validation of the research with Previous Studies**

| Comparison | Approach Used | Feature of Model | Accuracy of the Model |
|---|---|---|---|
| [12] | CNN Model | Pixel | 99.7% |
| [13] | Contact Process Model | Root Mean Square | 94.04% |
| [14] | ANN Model | Pixel | 96.8% |
| Proposed Model | CNN Model | Pixel | 98% |

### 3.2 Discussion

The images of some of the datasets are shown above. Based on the defects, six classes were created from the photos as: patches, scratches, pitted, rolled-in-scales, crazing, and inclusions. This was accomplished by obtaining a dataset of 1800 images of metal surfaces. With 300 photos of metal surfaces for each defect There are two categories for the system's accuracy training and validation. Research indicates that the implementation of artificial intelligence in assembly lines can effectively reduce time wastage. This is because the parts manufactured will go through the same process once the system is developed, negating the need to develop a new system. Furthermore, profilometers, which is a contact process, are expensive. Therefore, this research gives a solution for situations where batch size is relatively big and surface finish is a quality specification.

With the model established samples can be taken from production lines and compared accordingly. This can establish the surface finish as any of the six categories mentioned. Each of the surface value has a numerical value that can be appended as a range. The method makes the inspection process simpler, accurate and faster especially for continuous production process. The performance of the model is based on the ability to carry out correct classification and enlarged data size. Implementation challenges could include initial cost of purchase of cameras and association components, setup of computer laboratory for real time deployment and availability of trained personnels. It is however limited to applications where imaging is an important extraction factor.

## CONCLUSION

Surface roughness of a metal can be obtained through CNN after taking several surfaces and classifying them. The higher the number of the surfaces, the higher the accuracy obtained. CNN can be used to measure the surface roughness of a component and very useful on assembly line for continuous inspection proposes. This technique should be extended to the determination of friction resistance of metals and other surfaces. It can also be extended to the determination of the viscosity of a fluid, where change in colour is an important parameter.

## REFERENCES

1. Harlal, S., Mali, I., Ahamad, K., Anoj, M. & Mahammed, F. H. (2021). Machine vision for the measurement of machining parameters: A review. Through https//www.researchgate.net/publication/356735870
2. Seth Elder (2021). The basics of surface finish.
3. Anil, K. and Neeraj, K. (2020). Analysis of Surface Finishing Processes. *A Review,* 6.
4. Sharma, M. K. (2015). Analysis of effect on surface roughness and dynamic properties and performance on interface material contact stress area for vehicle engine.
5. Degarmo, E. P., Black, J. T. & Kohser, R. A. (2003). *Materials and Processes in Manufacturing,* (9th Edition). Wiley, ISBN 0-471-65653-4.
6. Abbot, Firster (2019). Roughness Parameter Evaluation. Science Direct.
7. Gadelmawla, E. S. & Koura, M. M. (2002). Roughness parameters. *Journals of material processing Technology*, 12(3), 133-145.
8. Amrit, K. (2022). Surface texture or finishing – definition, surface roughness methods.
9. ISO (1994). Quality Management and Quality Assurance: A Vocabulary. *International Organization for Standardization,* Geneva. Through; www.iso.org.
10. Ed Burns, N. & Laskowski, L. T. (2022). What is Artificial Intelligence.
11. W.A. Akpan, N.I. Effeng, C.M. Orazulume and E.J. Awaka-Ama Artificial Intelligence Based Quality Assurance of Surface Finish of Parts on Assembly Line Engineering and Technology Journal Volume 8, issue 9, pp 2685-2709.
12. Pronab Ghosh, Atqiya Abida Anjum, Asif Karim, Masum Shah Juayed, Md. Zahid Hassan, Khan Hasib, Al Nahian Bin Emran (2021): A Comparative Study of Different Deep Learning Model for Recognition of Handwriting Digits. SSRN Electronic Journal. DOI:10.2139/ssrn.3769231
13. Krzysztof, S. (2012). Statistical testing of the Measurement Accuracy of Mobile Roughness Measuring Profilometer. Kiele University of Technology, Poland.
14. Chen, S., Almamlook, R., Gu, Y & Wells (2018). Offline Handwriting Digits Recognition Using Machine Learning. Proceedings of the International Conference on Industrial Engineering and Operation Management, Washington DC, USA.